

G90577

A STUDY OF THE (p,d) REACTION
ON THE GERMANIUM ISOTOPES

By

David Lawrence Show

A DISSERTATION

Submitted to
Michigan State University
in partial fulfillment of the requirements
for the degree of

DOCTOR OF PHILOSOPHY

Department of Physics

1974

ABSTRACT

A STUDY OF THE (p,d) REACTION ON THE GERMANIUM ISOTOPES

By

David Lawrence Show

States in ^{69}Ge , ^{71}Ge , ^{72}Ge , ^{73}Ge and ^{75}Ge have been studied with the (p,d) reaction at a proton energy of 35 MeV. Deuterons were analyzed with an Enge split-pole magnetic spectrograph and detected in nuclear emulsions with an energy resolution of about 8 keV FWHM. Excitation energies were measured relative to a calibration calculated from the known characteristics of the spectrograph and previously well established excited state energies in the various nuclei. The resulting uncertainties were about 1.5 keV per MeV excitation. Angular distributions were measured between the angles of 6° and 60° . ℓ -transfer and spectroscopic factors were extracted by normalizing DWBA calculations to the angular distributions. These data allow the assignment of some spins and parities for the final states and the determination of the amount of filling of the active shell model orbits in the target nuclei.

ACKNOWLEDGMENTS

I would like to thank the entire Cyclotron staff for their assistance, without which these experiments could not have been possible. Specifically, the following people have been extra helpful:

My thesis adviser, Professor Hobson Wildenthal, for his indispensable counsel and guidance, and his wisdom to see when to let me wrestle on my own and when to come to my assistance;

Professor Jerry Nolen for his aid in setting up the Cyclotron for high resolution and for helpful discussions;

The plate scanners for their accurate and efficient scanning of the plates;

Richard Au and the computer staff for their assistance in maintaining good relations with the computer;

The National Science Foundation for its financial support during my work at the laboratory;

Finally, my wife for her moral and financial support and her tolerance of many lonely hours while I was working late or early.

TABLE OF CONTENTS

	Page
LIST OF TABLES.....	v
LIST OF FIGURES.....	vi
I. INTRODUCTION.....	1
II. EXPERIMENTAL PROCEDURE.....	7
II.1 Target Preparation.....	7
II.2 Proton Beam.....	7
II.3 Deuteron Detection.....	9
III. ANALYSIS OF DATA.....	19
III.1 Spectra Reduction.....	19
III.2 Excitation Energies.....	19
III.3 Normalization.....	21
III.4 DWBA Calculations and Fits.....	21
III.5 Spin-parity Assignments.....	25
IV. THE $^{70}\text{Ge}(p,d)$ REACTION.....	29
IV.1 General Comments.....	29
IV.2 Comments on Individual States.....	38
V. THE $^{72}\text{Ge}(p,d)$ REACTION.....	43
V.1 General Comments.....	43
V.2 Comments on Individual States.....	53
VI. THE $^{73}\text{Ge}(p,d)$ REACTION.....	58
VI.1 General Comments.....	58
VI.2 Comments on Individual States.....	69
VII. THE $^{74}\text{Ge}(p,d)$ REACTION.....	74
VII.1 General Comments.....	74
VII.2 Comments on Individual States.....	74
VIII. THE $^{76}\text{Ge}(p,d)$ REACTION.....	91
VIII.1 General Comments.....	91
VIII.2 Comments on Individual States.....	98

	Page
IX. DISCUSSION OF RESULTS.....	104
IX.1 General Features.....	104
IX.2 Summed Spectroscopic Factors.....	104
IX.3 Wave Functions.....	122
IX.4 Order of Filling of Orbits.....	126
X. SUGGESTIONS FOR FURTHER STUDY.....	128
LIST OF REFERENCES.....	130

LIST OF TABLES

Table		Page
1	Percentage isotopic contents of the target from the Oak Ridge National Laboratory separated isotopes division specification sheets.....	8
2	Summary of results for states in ^{69}Ge	30
3	Summary of results for states in ^{71}Ge	44
4	Summary of results for states in ^{72}Ge	59
5	Summary of results for states in ^{73}Ge	75
6	Summary of results for states in ^{75}Ge	92
7	Summed spectroscopic factors.....	119
8	Fractional fillings of orbits in the even isotopes.....	121

LIST OF FIGURES

Figure	Page
<p>1 Optical model predictions for the $^{72}\text{Ge}(p,p)$ reaction in the regions used for the absolute normalizations (upper curve) and for the monitor counter (lower curve). Boxes on the upper curve are experimental points from data taken for the absolute normalization of cross-sections for the $^{72}\text{Ge}(p,d)$ reaction.....</p>	11
<p>2 Sample spectra from the $^{70}\text{Ge}(p,d)$ and $^{72}\text{Ge}(p,d)$ reactions at 9° and 6° respectively. Energies shown are those obtained in the present work. Peaks due to germanium impurities are labelled with the mass number of the final nucleus.....</p>	14
<p>3 Sample spectra from the $^{73}\text{Ge}(p,d)$ and $^{74}\text{Ge}(p,d)$ reactions at 18° and 12° respectively. Energies shown are those obtained in the present work. Peaks due to germanium impurities are labelled with the mass number of the final nucleus.....</p>	16
<p>4 Sample spectrum from the $^{76}\text{Ge}(p,d)$ reaction at 15°. Energies shown are those obtained in the present work. Peaks due to germanium impurities are labelled with the mass number of the final nucleus.....</p>	18

Figure	Page
5 DWBA predications for ℓ -transfers of 1,3, and 4 at three excitation energies. The magnitudes have been normalized to correspond to an experimental angular distribution with a spectroscopic factor of one.....	24
6 Experimental angular distributions obtained from the $^{70}\text{Ge}(p,d)$ reaction at 35 MeV. The solid curves are fits to the data of DWBA predictions.....	35
7 Experimental angular distributions obtained from the $^{70}\text{Ge}(p,d)$ reaction at 35 MeV. The solid curves are fits to the data of DWBA predictions.....	37
8 Experimental angular distributions for three states observed in the $^{70}\text{Ge}(p,d)$ reaction at 25 MeV showing the $\ell=1$ j-dependence. The solid curves are drawn through the points to guide the eye.....	41
9 Experimental angular distributions obtained from the $^{72}\text{Ge}(p,d)$ reaction at 35 MeV. The solid curves are fits to the data of DWBA predictions.....	50
10 Experimental angular distributions obtained from the $^{72}\text{Ge}(p,d)$ reaction at 35 MeV. The solid curves are fits to the data of DWBA predictions.....	52

Figure	Page
11	Experimental angular distributions obtained from the $^{73}\text{Ge}(p,d)$ reaction at 35 MeV. The solid curves are fits to the data of DWBA predictions. For mixed ℓ -transfers, the dashed lines show the contribution of each component..... 66
12	Experimental angular distributions obtained from the $^{73}\text{Ge}(p,d)$ reaction at 35 MeV. The solid curves are fits to the data of DWBA predictions. For mixed ℓ - transfers, the dashed lines show the con- tribution of each component..... 68
13	Experimental angular distributions obtained from the $^{74}\text{Ge}(p,d)$ reaction at 35 MeV. The solid curves are fits to the data of DWBA predictions. For mixed ℓ -transfers, the dashed lines show the contribution of each component..... 82
14	Experimental angular distributions ob- tained from the $^{74}\text{Ge}(p,d)$ reaction at 35 MeV. The solid curves are fits to the data of DWBA predictions. For mixed ℓ -transfers, the dashed lines show the contribution of each com- ponent..... 84

Figure	Page	
15	Experimental angular distributions obtained from the $^{76}\text{Ge}(p,d)$ reaction at 35 MeV. The solid curves are fits to the data of DWBA predictions. For mixed ℓ -transfers, the dashed lines show the contribution of each component.....	97
16	Spectroscopic strength plotted as a function of excitation energy for ℓ -transfers of 1,3, and 4 for the (p,d) reaction on the even targets.....	106
17	Energy level diagram for states below 2 MeV in ^{69}Ge showing energy, ℓ -transfer, spectroscopic factor, and sample spectrum for states populated in the (p,d) reaction...	108
18	Energy level diagram for states below 2 MeV in ^{71}Ge showing energy, ℓ -transfer, spectroscopic factor, and sample spectrum for states populated in the (p,d) reaction.....	110
19	Energy level diagram for states below 3.5 MeV in ^{72}Ge showing energy, ℓ -transfer, spectroscopic factor, and sample spectrum for states populated in the (p,d) reaction.....	112

Figure	Page
20	Energy level diagram for states below 2 MeV in ^{73}Ge showing energy, ℓ -transfer, spectroscopic factor, and sample spectrum for states populated in the (p,d) re- action..... 114
21	Energy level diagram for states below 2 MeV in ^{75}Ge showing energy, ℓ -transfer, spectroscopic factor, and sample spectrum for states populated in the (p,d) re- action..... 116

I. INTRODUCTION

The nuclear shell model treats the nucleus as a small number of "active" nucleons moving in a potential produced by the remaining "core" nucleons. In its simplest form the nucleons fill one "orbit" after another in a prescribed order and these orbits are grouped into shells. Each orbit is described by its principle quantum number, orbital angular momentum, (l) and total spin ($j = l \pm 1/2$) so that the representation for the first orbit with three units of orbital angular momentum and total spin of $5/2$ would be $1f_{5/2}$. The total number of protons and neutrons allowed in a given orbit is restricted to $2j+1$ each. This model has been used with considerable success, especially near filled shells and in the p and s-d shells. With these successes there is a growing interest in applying it to the upper f-p shell, which is comprised of the $2p_{3/2}$, $1f_{5/2}$, $2p_{1/2}$, $1g_{9/2}$ orbits and includes the germanium isotopes. In the past, attempts have been made at applying the rotational model to this region, but without much success.^{1,2)}

In order to facilitate a shell model calculation it is desirable to have available considerable experimental information of the type that can be obtained from single particle transfer experiments. Included are:

1. Excitation energies. Once the energies of the

emitted reaction particles are measured, it is a simple matter to calculate excitation energies from the incident beam energy, the reaction ground-state Q -value, and the reaction kinematics.

2. Orbital angular momenta of transferred particles. It has long been known that in particle-transfer experiments a plot of the probability of populating a given state as a function of the scattering angle has a shape characteristic of the ℓ -value of the transferred particle. By making such plots (called angular distributions) for all the states observed, it is possible to determine which orbits contain nucleons (neutrons for (p,d) and (d,p) reactions) in the target nucleus. This in turn yields information about the wave function of the target nucleus. Information is also obtained about the wave functions of the final states. Parities are determined, since they are the same as that of the target nucleus for even- ℓ transfer and opposite for odd- ℓ transfer. In addition, restrictions are placed on the spins of the final states since they must be vector sums of the target total angular momentum and the total angular momentum of the transferred particles. In most cases, the angular distributions are not significantly dependent upon the total angular momentum of the transferred particle, so that in general "j-transferred" cannot be experimentally determined

directly. The exception is the case of an $\ell=0$ transfer, in which case the j -transferred must be $1/2$. If the target spin is not zero, the spin of the final state is not significantly restricted by the determination of ℓ , especially if the target spin is large ($j \geq 2$) and the ℓ -transfer is greater than 1. On the other hand, if the target spin is zero, as is often the case, the spin of the final state is restricted to two possibilities regardless of the ℓ -transfer, and there are sometimes reasons for preferring one over the other so that tentative spin assignments can be made.

3. Spectroscopic factors. Further information is available from the overall probability of populating a final state. By taking the ratio of the experimental intensity of a transition to the Distorted Wave Born Approximation (DWBA) prediction for the intensity, one extracts a number called the spectroscopic factor. This again gives information about both the target nucleus and the final state. The sum of the spectroscopic factors for a given ℓ - j transfer is a measure of the total population of that orbit in the target nucleus (assuming that all the states that can be populated by that ℓ - j transfer are observed). The individual spectroscopic factors are a measure of the overlap of the target state wave function with the final state wave function plus (or minus) a particle

of the appropriate ℓ - j . For example, in the (p,d) reaction a large spectroscopic factor indicates a wave function for the final state that is just the target wave function with one neutron removed, while a small spectroscopic factor indicates further rearrangement or recoupling between the particles in the target and in the final state or that no particles of that ℓ - j are present in the target.

Information of types 2) and 3) are useful in determining which orbits must be considered in the active space of a shell model and perhaps whether the calculation is even feasible, since an active space that is too large becomes impossible to use because of finite computer size and time.

Experimentalists have recently shown an increasing interest in the upper f-p shell mass region, in particular the germanium isotopes. The γ -decays of these nuclei have been studied by Hasselgren and by Weishaupt et al., with the (n, γ) reaction,^{3,4)} by Malan et al. with the (p,n γ) reaction,^{5,6)} by Salzman et al. with the (α , α' γ) reaction,⁷⁾ by Jones et al. by stopping ⁷³Ge ions in germanium,⁸⁾ and by Murray et al., Van Hise et al., Muszynski et al., Chen, et al., Camp et al., and Rester et al. in β -decay experiments.^{9-13,2)} The results of these experiments provide accurate excitation energies and, for some states, spin-parity assignment or limitations. Particle transfer experiments that have been performed include those of Goldman, Heyman

et al., Hasselgren, and Kato using the (d,p) reaction^{14,15,3,16} and of Hsu, et al. and Fournier, et al. using the (p,d) reaction.^{17,18}) It is expected that the structure of the low-lying states in the odd isotopes is predominately determined by the neutrons due to the presence of an unpaired neutron. For this reason, the neutron transfer experiments should be essential for studying these states.

The present work was undertaken to refine and extend the previous neutron transfer experiments on the germanium isotopes. The MSU Cyclotron Laboratory is especially well equipped for (p,d) experiments because of its high quality proton beam and the Enge split-pole magnetic spectrograph. Using dispersion-matching techniques it has become a routine procedure to get deuteron spectra with a resolution of better than 10 keV FWHM at a bombarding energy of 35 MeV. This type of good resolution is highly desirable if accurate results are to be obtained in the present experiment, for two reasons. First, the level structure of the odd germanium isotopes is fairly dense, with several cases where the level separation is less than 15 or 20 keV. Second, in the region of excitation above 2.5 or 3 MeV the levels are usually weakly populated and the high resolution helps considerably in causing these levels to stand out from any background that may be present. Hasselgren³⁾ has obtained an energy resolution of about 8 keV in the (d,p) reaction while the best resolution previously obtained in the (p,d) reaction was about 35 keV by Fournier et al.¹⁸⁾ Our high resolution (p,d) data can

be expected to clear up many ambiguities attendant in the previous poorer resolution.

II. EXPERIMENTAL PROCEDURE

II.1 Target Preparation

The germanium used for making the targets was obtained from Oak Ridge National Laboratory in the form of GeO_2 . Table 1 shows the quoted relative abundances of each of the five stable germanium isotopes in the material used for each target. The standard techniques for forming the targets are outlined as follows:

1. Carbon foils ($\sim 25 \text{ } \mu\text{g}/\text{cm}^2$) were floated on water and then picked up so as to cover a $3/4$ " hole in an aluminum frame.
2. About 8 mg of GeO_2 was placed in a $1/4$ " I.D. tantalum tube with both ends crimped and a hole (.012" diameter) drilled midway between the ends.
3. The tube and target frame were mounted in a vacuum evaporator and by passing a current of about 200 amps through the tube the GeO_2 was evaporated onto the carbon at an evaporating distance of about 2 cm.

This procedure resulted in targets that were very uniform and about $175 \text{ } \mu\text{g}/\text{cm}^2$ thick.

II.2 Proton Beam

The targets were bombarded with the 35 MeV proton beam from the MSU cyclotron. Currents were in the range from 400 to 700 nanoamps. The energy of the beam was measured

Table 1. Percentage isotopic contents of the targets from the Oak Ridge National Laboratory separated isotopes division specification sheets.

Target	^{70}Ge	^{72}Ge	Isotope ^{73}Ge	^{74}Ge	^{76}Ge
" ^{70}Ge "	84.62	5.54	1.47	6.36	2.01
" ^{72}Ge "	2.70	90.88	1.27	4.23	0.93
" ^{73}Ge "	2.14	5.06	85.58	6.61	0.62
" ^{74}Ge "	1.71	2.21	0.90	94.48	0.70
" ^{76}Ge "	7.69	6.65	1.69	10.08	73.89

using two calibrated 45° bending magnets in the beam transport system, with slits before, between, and after the magnets. A typical measured value for the energy was 35.050 MeV, accurate to ~ 25 keV.

After passing through the target, the protons were collected in a Faraday cup connected to a charge integrator which monitored beam current and total charge. These data were used for relative normalization of the cross sections from one angle to another. Elastically scattered protons were detected in a NaI detector (monitor counter) mounted at 90° with respect to the beam. These data were used as a check on the normalization determined from the Faraday cup and in the cross section normalization procedure.

The lower part of Figure 1 shows the DWBA prediction for elastic scattering from ^{72}Ge in the region of 90° . Since there is a peak in the cross section near 90° the monitor data can be expected to be stable against small changes in the beam position on the target.

II.3 Deuteron Detection

The deuterons were analyzed in an Enge split-pole magnetic spectrograph and detected in nuclear emulsions placed in the focal plane of the magnet. Using dispersion matching techniques a resolution of about 8 keV FWHM was obtained for most of the spectra from the plate data. The plates were scanned with the aid of a computer-linked microscope system that facilitated scanning in .1 mm steps and in the

Figure 1. Optical model predictions for the $^{72}\text{Ge}(p,p)$ reaction in the regions used for the absolute normalizations (upper curve) and for the monitor counter (lower curve). Boxes on the upper curve are experimental points from data taken for the absolute normalization of cross-sections for the $^{72}\text{Ge}(p,d)$ reaction.

$^{72}\text{Ge}(p,p)$

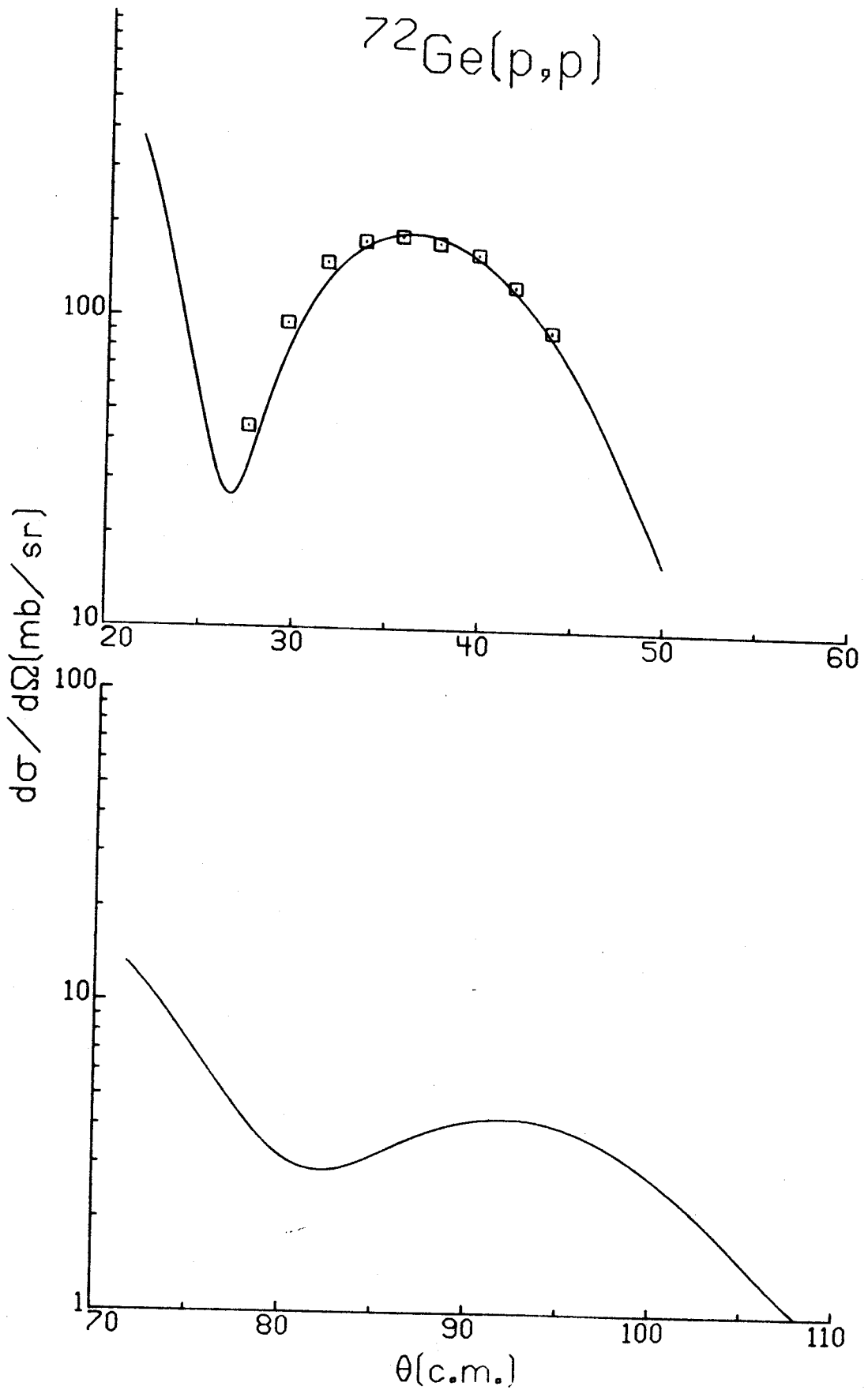


Figure 1

straightening out of the tilted images on some plates. The small step size is necessary because the high quality of the data produces peaks that are only about .3 mm wide, FWHM, and a larger step size would prevent observation of peak broadening in the case of closely spaced doublets. Typical spectra for each of the targets are shown in Figures 2-4. In all of the experiments with plates, two plates were placed end to end in the focal plane of the spectrograph. The spectra shown in the figures are from the first plate only. The second plate was used primarily to determine if there were any strong peaks at high excitation energies. Supplementary data was also taken using a position-sensitive wire proportional counter instead of the plates, but the counter-limited resolution of about 60 keV severely restricted the use of these data, except for cross section normalization purposes. In connection with the normalization process we took angular distributions of the elastically scattered protons in the region of the maximum at about 35° . The use of these data will be described in the next chapter.

Figure 2. Sample spectra from the $^{70}\text{Ge}(p,d)$ and $^{72}\text{Ge}(p,d)$ reactions at 9° and 6° respectively. Energies shown are those obtained in the present work. peaks due to germanium impurities are labelled with the mass number of the final nucleus.

Figure 3. Sample spectra from the $^{73}\text{Ge}(p,d)$ and $^{74}\text{Ge}(p,d)$ reactions at 18° and 12° respectively. Energies shown are those obtained in the present work. Peaks due to germanium impurities are labelled with the mass number of the final nucleus.

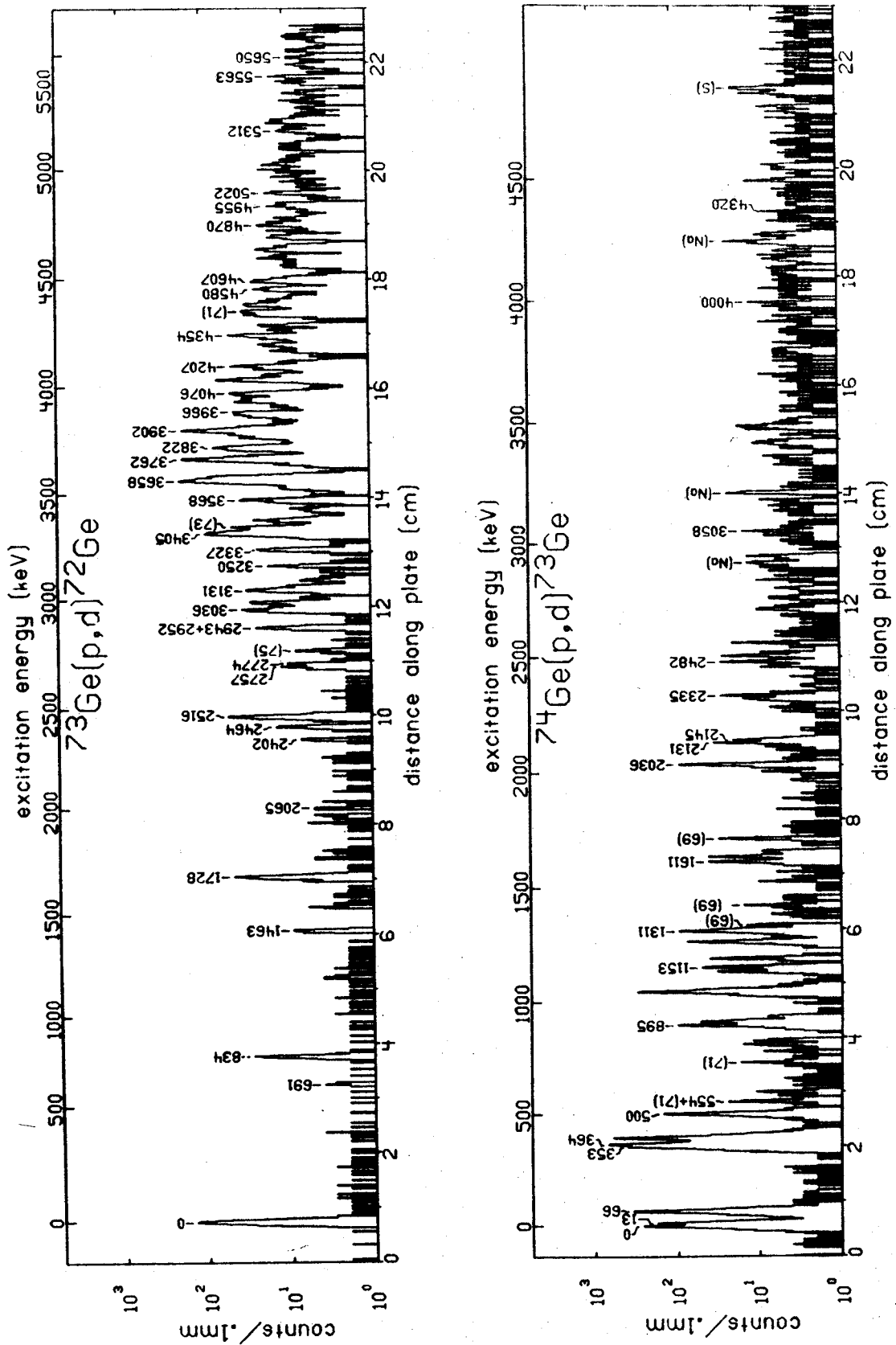


Figure 3

5

Figure 4. Sample spectrum from the $^{76}\text{Ge}(p,d)$ reaction at
Energies shown are those obtained in the present
work. Peaks due to germanium impurities are
labelled with the mass number of the final
nucleus.

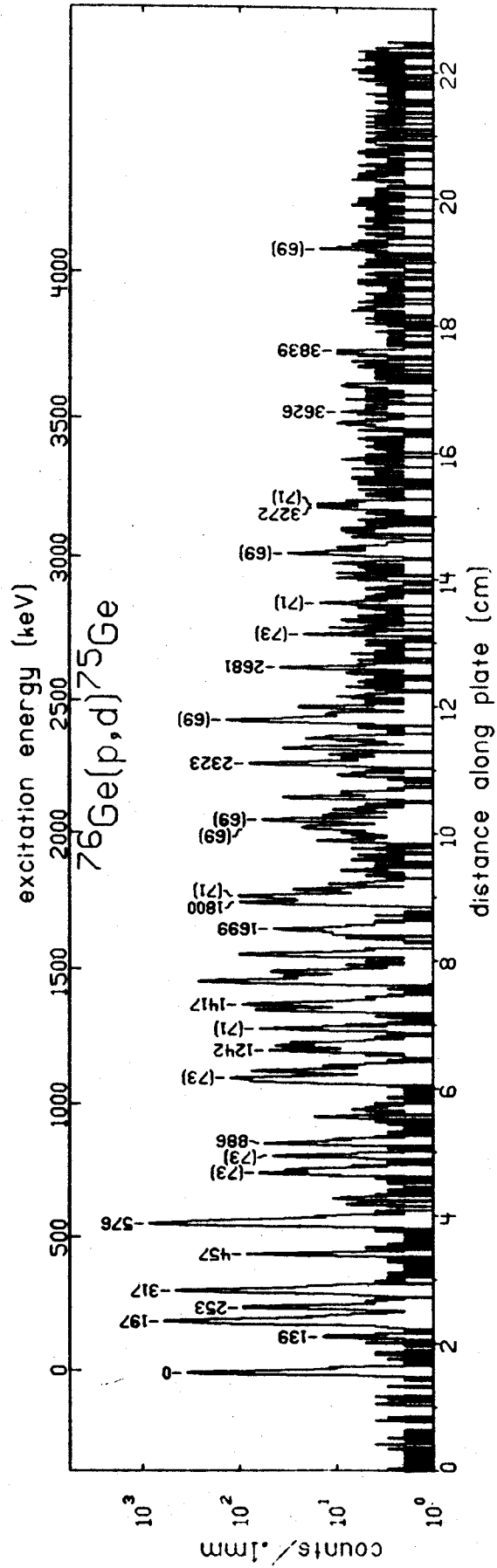


Figure 4

III. ANALYSIS

III.1 Spectra Reduction

The computer code Sampo¹⁹⁾ was used to extract peak positions and peak areas from the spectra. This code fits a gaussian shape whose parameters are determined from a chosen peak to all the peaks and gives centroids and integrated counts. This type of fitting procedure is indispensable for cases in which the energy separation between two states is close to the limit of our resolution and the peaks are not completely separated.

III.2 Excitation Energies

The excitation energies reported for this work were calculated with the aid of the computer code Monster.²⁰⁾ The parameters of the calculation include beam energy, spectrograph field strength, observation angle, focal plane position, peak centroids and areas, centroids and energies of calibration peaks, and reaction Q-value. Calibration peaks are those corresponding to states whose energies are well known (<1 keV uncertainties) regardless of the reaction that produced them. Typical calibration peaks in the present experiment were the ground state and strong excited states of any germanium isotope observed, and the ground state of ^{31}S from the $^{32}\text{S}(p,d)$ reaction. The excitation energies used for the germanium calibration peaks are those from γ -ray

experiments. These calibration peaks were spaced along most of the plate.

Monster uses the known ρ vs. D characteristics of the spectrograph in conjunction with these calibration peaks to determine the excitation energy of each peak given. Since the program allows input of the Q -values for the various reactions, these can be adjusted to give the best fit to the calibration peaks. This allows us to compensate for small errors in the Q -values calculated from the mass tables of Wapstra and Gove²¹⁾ which would otherwise ruin the calibration. In the ^{70}Ge and ^{76}Ge targets there was sufficient contamination with the other germanium isotopes to allow the determination of relative Q -values for all the reactions except the $^{73}\text{Ge}(p,d)$ reaction. However, since ^{74}Ge , ^{73}Ge , and ^{72}Ge are all stable, their masses are well known and hence the $^{74}\text{Ge}(p,d)$ and $^{73}\text{Ge}(p,d)$ reaction Q -values were assumed to be correct and the others were adjusted as needed. In all cases the adjustments needed were within the limits of the quoted uncertainties in the masses of the other odd isotopes. The uncertainty in the excitation energies calculated in this work is about 1.5 keV/MeV excitation. For the purposes of plotting the angular distributions, Monster also calculates the center of mass scattering angle and cross section.

III.3 Normalization

As was previously mentioned, the relative angle to angle normalization for the data on a given target was done using the integrated charge from the Faraday cup. In comparing the monitor counter normalization with this method, they were found to agree within 5%.

For the purpose of establishing a cross section scale we used proton elastic scattering angular distributions. These data were normalized to optical model calculations made with the proton parameters of Becchetti-Greenlees.²²⁾ The data and calculation for ^{72}Ge are shown in the top part of Figure 1 and indicate a good fit to the data by the theoretical curve. Assuming the optical model predictions to be correct, we can now use the normalization factor thus obtained to convert counts in the wire-counter per count in the monitor counter to mb/sr. Since deuteron spectra were taken under identical conditions we thus have a cross section normalization factor for the deuteron angular distributions. This procedure yields an estimated experimental uncertainty of about 20% in the absolute spectroscopic factors.

III.4 DWBA Calculations and Fits

All DWBA calculations were made with the computer code DWUCK²³⁾ and made use of its approximate finite range and nonlocality correction options. The proton parameters used

were those of Becchetti-Greenlees²²⁾ and the deuteron parameters were calculated from the Becchetti-Greenlees proton and neutron parameters according to the adiabatic model of Johnson and Soper²⁴⁾ with Satchler's prescription.²⁵⁾ Figure 5 shows the calculated shapes for ℓ -transfers of 1, 3, and 4 at three excitation energies. In fitting the theory to the data, a minimum χ^2 procedure was used which considered only the angular range from 0° to 32° . The resulting fits show good agreement between data and theory. At higher excitation energies there is a discrepancy in the $\ell=3$ fits, as the calculations show a dip at forward angles while the data maintains the shape of the low lying $\ell=3$ transitions.

There is occasionally some ambiguity in making ℓ -assignments. For example, a mixture of $\ell=1+4$ may fit a given transition in the $^{73}\text{Ge}(p,d)$ reaction about as well as an $\ell=1+3$ mixture, particularly if the $\ell=1$ component dominates the transition. In such cases we have preferred the $\ell=1+3$ assignment since an $\ell=1+4$ mixture would require the final state to actually be a doublet because of the different parity associated with the two components. In the case of the even targets, any mixture of ℓ 's implies a doublet (because of different spins or different parities) and we have not attempted fitting with a mixture unless there is strong evidence for it.

Figure 5. DWBA predictions for ℓ -transfers of 1,3, and 4 at three excitation energies. The magnitudes have been normalized to correspond to an experimental angular distribution with a spectroscopic factor of one.

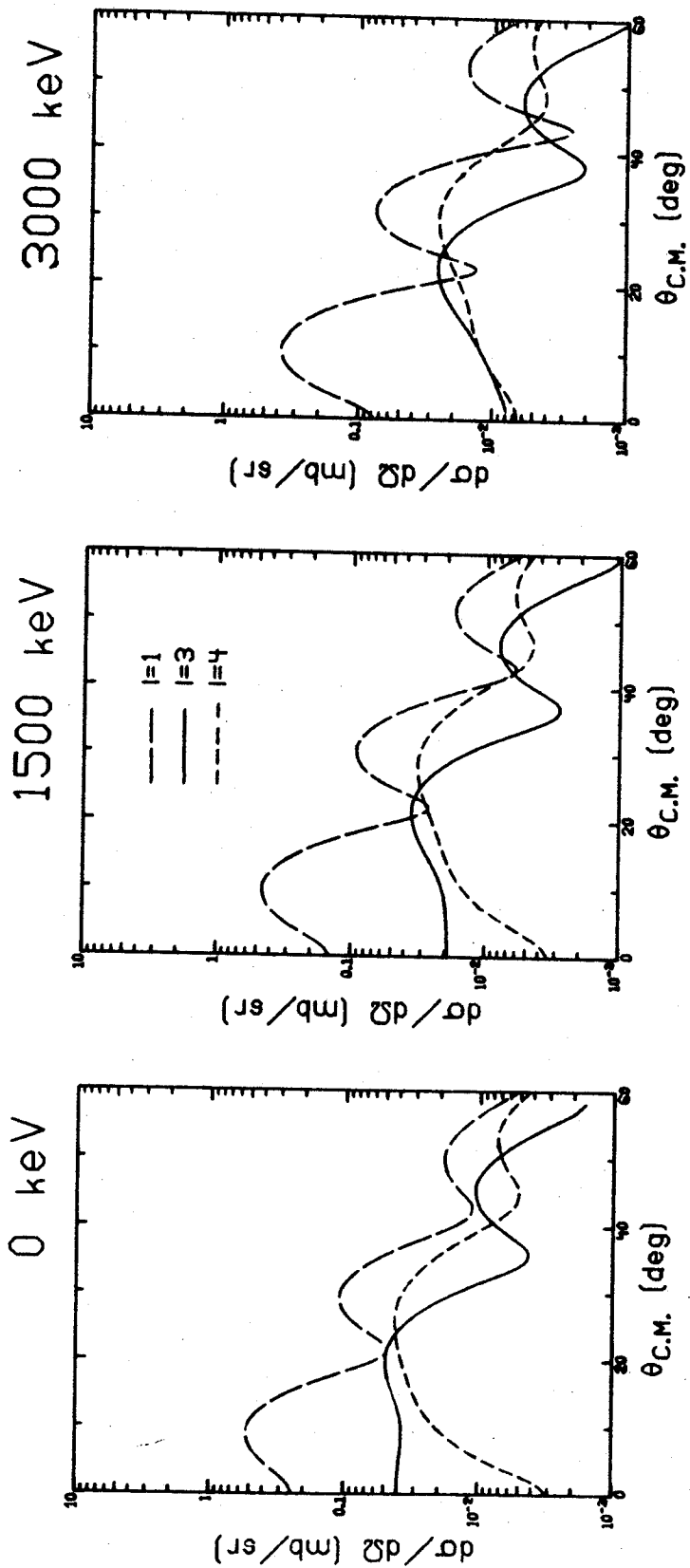


Figure 5

d 4
es
tro-

III.5 Spin-Parity Assignments

The parity of any state is uniquely determined by the ℓ -transfer of the transition to that state. Since all the target states in the present experiment have positive parity, the parity of a final state is positive for an even ℓ -transfer and negative for odd ℓ -transfer.

In most cases it is not possible for us to make definite spin assignments since we cannot measure the spins of the transferred neutrons except for $\ell=0$ transitions. The situation is complicated even more for the $^{73}\text{Ge}(p,d)$ reaction since the spin of the ground state is not zero and even if we knew the spin of the transferred neutron we would not know the spin of the final state. We can make spin assignments for states in ^{72}Ge in the occasional cases where γ -decay experiments have limited the spin to two or three possibilities and our results are consistent with only one of these. For the odd isotopes we can make tentative spin suggestions for most of the states based on the following considerations.

1. All states populated via $\ell=2$ transfer are assumed to have a spin of $5/2$. In order to have a state with $J=3/2$ populated with an $\ell=2$ transfer we would have to pick up a neutron from the $1d_{3/2}$ orbit or the $2d_{3/2}$ orbit. The former should only occur (if at all) for states at high excitation energy since the $1d_{3/2}$ orbit is two shells below the f-p shell. Pickup from the $2d_{3/2}$ orbit could occur but it is doubtful that this

orbit is significantly populated in the target nuclei. The $2d_{5/2}$ orbit should fill appreciably before any filling of the $2d_{3/2}$ orbit began. We see very little $\ell=2$ strength which indicates that even the $2d_{5/2}$ orbit is not populated to any significant extent.

2. All states populated via $\ell=3$ transfer are assumed to have a spin of $5/2$. We might expect to see some pick-up from the $1f_{7/2}$ orbit which would yield states with $j=7/2$. These states would be expected to occur at a fairly high excitation energy since the $1f_{7/2}$ shell is well below the higher orbits populated in energy, and we would expect most of the $J=5/2^-$ states to be lower in excitation energy than these $J=7/2^-$ states. The fact that we do not see enough $\ell=3$ strength to exceed the sum rule limit for $1f_{5/2}$ pickup tends to indicate that we see little if any $1f_{7/2}$ pickup. However, we cannot rule out the possibility that some of the higher excited states that we observe to be populated by $\ell=3$ transfer may actually be $7/2^-$ states, or that some of the weakly populated states may be $7/2^-$ states whose wave functions are dominated by $(1f_{5/2})^3$ etc. configurations.

3. All states populated via $\ell=4$ transfer are assumed to have spin $9/2$. There is one exception to this and that is the case of the 139 keV state in ^{75}Ge which is known to have $J=7/2^{26)}$ This exception indicates that

at least in ^{76}Ge there is some filling of the $1g_{7/2}$ orbit. There are also possible $7/2^+$ states in both ^{71}Ge (7) and ^{73}Ge (29) which we do not observe. The state in ^{71}Ge is definitely not populated to an observable degree while the state in ^{73}Ge would be obscured in our data by a strong $\ell=1$ transition to a state less than 2 keV away. Any pickup from the $1g_{7/2}$ orbit would be expected to populate states generally lower in excitation energy than pickup from the $1g_{9/2}$ orbit since the $1g_{7/2}$ orbit is one shell lower than the $1g_{9/2}$ orbit. All the other states in these nuclei below 1 MeV excitation that are populated by an $\ell=4$ transfer in the (p,d) reaction are known to be $9/2^+$ states, therefore the few $\ell=4$ transitions to higher excited states that we observe are quite likely due to $1g_{9/2}$ pickup.

4. The states populated via $\ell=1$ transfer present a much more difficult problem. Both the $2p_{2/3}$ and $2p_{1/2}$ neutron orbits are partially filled in the germanium isotopes and they are close together in energy. Therefore we can at best make a slight preference for one spin over the other. The $2p_{1/2}$ orbit is slightly higher than the $2p_{3/2}$ orbit so in general the simplest shell model picture predicts the $1/2^-$ states should occur at lower excitation energies than the $3/2^-$ states. On this basis we have preferred a spin of $3/2$ for $\ell=1$ transitions to states above 1 MeV excitation.

The application of a general argument to this specific case suggests that since the $2p_{3/2}$ orbit should be mostly filled and the $2p_{1/2}$ orbit only partially filled, a strong (d,p) transition coupled with a weak (p,d) transition indicates a $1/2^-$ state while the reverse situation indicates a $3/2^-$ state. The data for the low-lying states with well known spin supports this argument and we have used it where it is applicable. However, the summed spectroscopic factors indicate that both orbits are about half full rather than the $2p_{3/2}$ orbit being almost full and the $2p_{1/2}$ orbit being mostly empty. It therefore appears that the $3/2^-$ and $1/2^-$ spin suggestions based on the (p,d) and (d,p) data must be regarded as very tenuous. It should be noted that the spectroscopic factors for $\ell=1$ transitions extracted in this work are independent of the spin transfer since the spin-orbit force is not strong enough to produce an appreciable difference in the calculated cross sections.

IV. THE $^{70}\text{Ge}(p,d)^{69}\text{Ge}$ REACTION

IV.1 General Comments

The absolute normalization of the cross sections for this reaction was obtained with a procedure different than that employed for the other reactions. For this case the normalization was calculated from the isotopic abundances of ^{70}Ge , ^{72}Ge , and ^{74}Ge in the respective targets and the absolute normalizations for the $^{72}\text{Ge}(p,d)$ and $^{74}\text{Ge}(p,d)$ reactions. This less direct procedure probably accounts for the fact that the sum of all the spectroscopic factors for this reaction exceeds the expected limit by about 25%, while for all the other isotopes the sum is slightly less than the limit. For the purpose of comparing the fractional fillings of the orbits we have normalized the sum for this isotope to the limit.

The results for this reaction are summarized in Table 2 and the angular distributions are shown in Figures 6 and 7. In general, where it is possible to make comparisons we find good agreement between the excitation energies, l -values, and spectroscopic factors obtained in the present study and those of previous work. In addition, many new states and their characteristics are also observed in the present work about which nothing was previously known. The second plate for this reaction showed no peaks stronger than 20 $\mu\text{b}/\text{sr}$ at 6° between 3.8 MeV and 7 MeV excitation.

Table 2. Summary of results for states in ^{69}Ge .

E_x (keV)	$^{70}\text{Ge}(p,d)$ Present Work		$^{70}\text{Ge}(p,d)$ Hsu et al. ¹⁷⁾		γ -ray Muszynski ¹¹⁾		Combined Results for ^{69}Ge	
	ℓ	C^2S	ℓ	C^2S	J^π	J^π	E_x (keV) ^{c)}	J^π
0	3	3.80	3	2.56	$5/2^-$	$5/2^-$	0	$5/2^-$
87	1	.56	1	.5		$1/2^-$	86.8	$1/2^-$
233	1	.10	1	.09		$3/2^-$	232.7	$3/2^-$
374	1	1.67	1	1.64		$3/2^-$	374.1	$3/2^-$
398	4	.95	4	.8	$9/2^+$	$9/2^+$	398.1	$9/2^+$
813	2	.09	1+3	.05, .27	$5/2^+$		813±2	$5/2^+$
995	1	.32	1+4	.06, .29	$1/2^-$		995±2	$1/2^-$
1159	1	.06	1	.26	weak		1159±2	$3/2(1/2)^-$
1278 ^{a)}	1	.02		weak			(1212±6)	
1306	1	.08	1	.1	$3/2(1/2)^-$	$3/2(1/2)^-$	1278±2	$3/2(1/2)^-$
(1406) ^{a)}	1	.08	1	.1	$3/2(1/2)^-$	$3/2(1/2)^-$	1306±2	$3/2(1/2)^-$
1414	3	.28	(3)	.35	$5/2^-$		(1406±2)	
1438 ^{a)}	3	.28	(3)	.35	$5/2^-$		1414±2	$5/2^-$
1468 ^{a)}	4	.09			$9/2^+$		1438±2	
1477	3	.96	(3)	1.12	$9/2^+$		1468±5	$9/2^+$
					$5/2^-$		1477±4	$5/2^-$

Table 2 - Continued.

E_x (keV)	$^{70}\text{Ge}(p,d)$ Present work		$^{70}\text{Ge}(p,d)$ Hsu et al. ¹⁷⁾		γ -ray Muszynski ¹¹⁾		Combined Results for ^{69}Ge E_x (keV) ^{c)}	
	ℓ	C^2S	ℓ	C^2S	J^π	J^π	J^π	J^π
1537 ^{a)}	1	.03						1537 \pm 4
1611	3	.25		weak				1611 \pm 4
1724 ^{a)}	1	.03						1724 \pm 4
1763	0	.12		weak				1763 \pm 4
1887 ^{a)}	1	.02						1887 \pm 8
1919				weak				1919 \pm 5
1989	2	.02		weak				1989 \pm 5
2012 ^{a)}								2012 \pm 5
2091 ^{a)}	0	.02						2091 \pm 4
2106	1	.16	1	.17				2106 \pm 4
2145	4	.30		weak				2145 \pm 4
2194	1	.03		weak				2194 \pm 4
2350 ^{a)}	3	.15						2350 \pm 4
2359	1	.04		weak				2359 \pm 4
2370 ^{a)}	3	.08						2370 \pm 4
2395	(4)	.22		weak				2395 \pm 4
2458				weak				2458 \pm 4

Table 2 - Continued.

E_x (keV)	$^{70}\text{Ge}(p,d)$ Present Work		$^{70}\text{Ge}(p,d)$ Hsu et al. (17)		γ -ray Muszynski (11)		Combined Results for ^{69}Ge (b)	
	λ	C^2S	J^π	λ	C^2S	J^π	E_x (keV) (c)	J^π
2500							2500 \pm 5	
2617 ^{a)}	1	.01	3/2(1/2) $^-$		weak		2617 \pm 5	3/2(1/2) $^-$
(2637)							2637 \pm 10	
2741	1	.1	3/2(1/2) $^-$		weak		2741 \pm 7	3/2(1/2) $^-$
2765 ^{a)}	3	.12			weak		2765 \pm 7	5/2 $^-$
2812 ^{a)}	1	.03	3/2(1/2) $^-$				2812 \pm 7	3/2(1/2) $^-$
2853* ^{a)}	3	.08	5/2 $^-$				2853* \pm 7	5/2 $^-$
2959 ^{a)}	1	.02	3/2(1/2) $^-$				2959 \pm 5	3/2(1/2) $^-$
2985 ^{a)}	(2)	.03	(5/2 $^+$)				2985 \pm 5	(5/2 $^+$)
3073 ^{a)}	2	.02	5/2 $^+$				3073 \pm 5	5/2 $^+$
3173 ^{a)}	3	.18	5/2 $^-$				3173 \pm 5	5/2 $^-$
3232 ^{a)}	1	.02	3/2(1/2) $^-$				3232 \pm 5	3/2(1/2) $^-$
3374 ^{a)}							3374 \pm 5	
3410 ^{a)}	3	.09	5/2 $^-$				3410 \pm 5	5/2 $^-$
3460 ^{a)}	(4)	.13	(9/2 $^+$)				3460 \pm 5	(9/2 $^+$)
3482 ^{a)}							3482 \pm 5	
3615 ^{a)}	1	.01	3/2(1/2) $^-$				3615 \pm 7	3/2(1/2) $^-$

Table 2 - Continued.

E_x (keV)	$^{70}\text{Ge}(p,d)$ Present Work		$^{70}\text{Ge}(p,d)$ Hsu et al. ¹⁷⁾		γ -ray Muszynski ¹¹⁾		Combined Results for ^{69}Ge ^{b)}	
	ℓ	C^2S	J^π	ℓ	C^2S	J^π	E_x (keV) ^{c)}	J^π
3622 ^{a)}							3622 \pm 7	
3680 ^{a)}	1	.02	$3/2(1/2)^-$				3680 \pm 7	$3/2(1/2)^-$
3729 ^{*a)}							3729 \pm 7	
3798 ^{*a)}	3	.22	$5/2^-$				3798 \pm 7	$5/2^-$
3828 ^{a)}							3828	

* Doublet.

a) States observed for the first time in the present work.

b) Compiled from the results of the present work and those of References 11 and 17.

c) Uncertainties are ± 1 keV for states quoted to a tenth of a keV.

Figure 6. Experimental angular distributions obtained from the $^{70}\text{Ge}(p,d)$ reaction at 35 MeV. The solid curves are fits to the data of DWBA predictions.

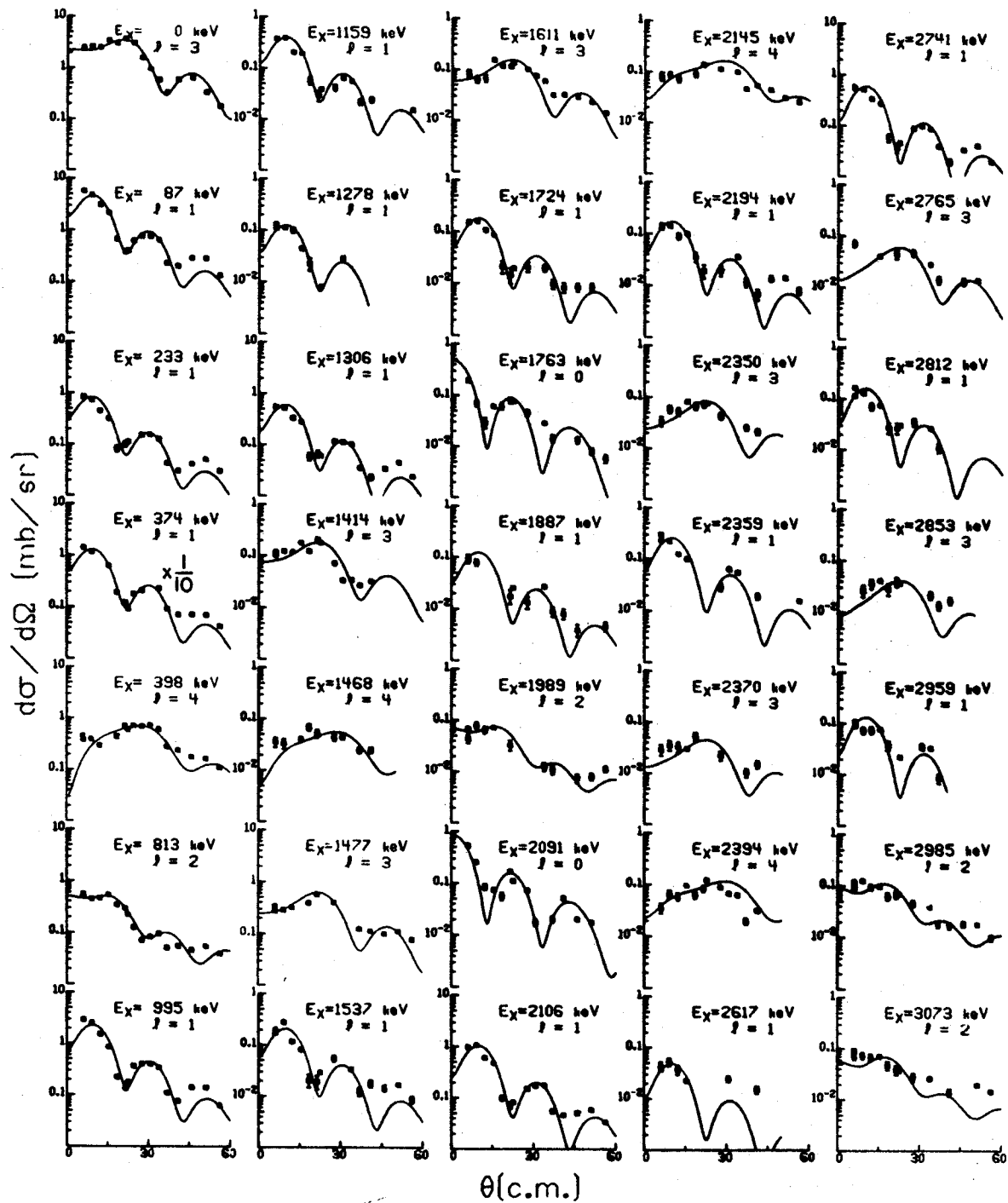


Figure 6

Figure 7. Experimental angular distributions obtained from the $^{70}\text{Ge}(p,d)$ reaction at 35 MeV. The solid curves are fits to the data of DWBA predictions.

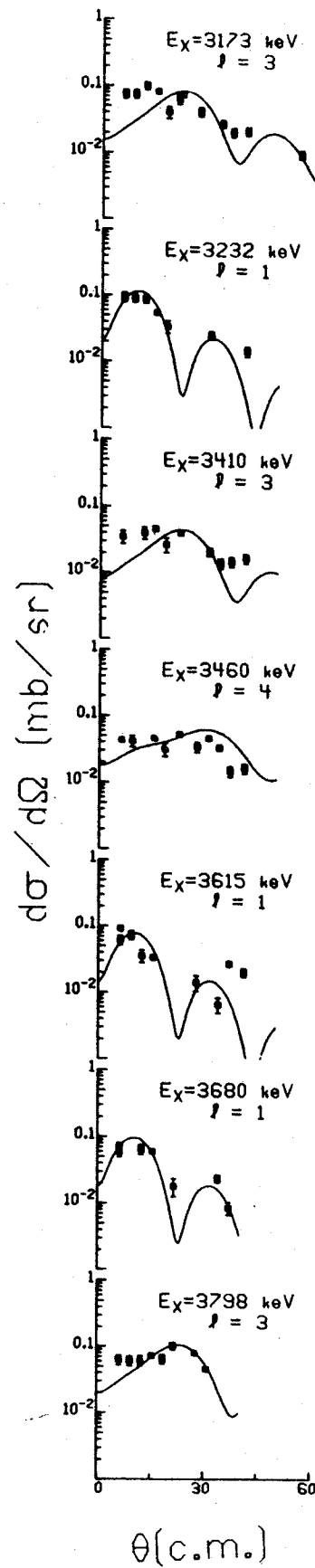


Figure 7

The distribution of the strong transitions in the (p,d) reaction on the germanium isotopes is shown in Figure 16. The $^{70}\text{Ge}(p,d)$ reaction is typical in this respect and shows the following: there is a strongly populated $1/2^-$ state near or at the ground state, a stronger $3/2^-$ state in the 400-600 keV range, and a moderately strong $1/2^-$ state at about 1 MeV. The $\ell=3$ strength is mostly concentrated in a single state below 400 keV with two or three weaker states at about 1.4 MeV. A single state near or at the ground state carries almost all the $\ell=4$ strength with the rest scattered along the spectrum in two or three weak states.

For the purposes of comparing our results with those reported for the (p,d) reaction by Hsu et al.¹⁷⁾ and Fournier et al.¹⁸⁾ it is useful to point out that the isotopic purities of the targets used in the present work are comparable to those used in the previous work. Thus, impurity peaks from germanium isotopes other than the one with which the target is enriched should be populated with approximately the same strength in both experiments.

IV.2 Comments on Individual States

813 keV state: The angular distribution that we obtain for this state shows a pure $\ell=2$ shape. Hsu et al.¹⁷⁾ were unable to fit the angular distribution for this state well and show attempted fits with both $\ell=1+3$ and $\ell=1+4$ mixtures. The data of reference 17 for this state are of low statistical

accuracy and do not permit discrimination between these mixtures. Our data, with better statistics, removes the previous ambiguity and also removes any need for calling this state a doublet, which would arise with a mixed ℓ -transfer. The resulting $5/2^+$ assignment for this state is consistent with the systematics seen in the other odd nuclei in which at least one $5/2^+$ state is always seen below 1 MeV excitation.

995 keV state: We have made an attempt to determine the feasibility of making spin assignments for the $\ell=1$ transitions by the J -dependence as described by Lee and Schiffer.²⁷⁾ For this purpose we measured differential cross sections of the $^{70}\text{Ge}(p,d)$ and $^{60}\text{Ni}(p,d)$ reactions at a bombarding energy of 25 MeV in the angular range of 60° to 90° . These data were taken with the position-sensitive wire proportional counter, the resolution of which (~ 40 keV FWHM at this energy) only allowed us to resolve a few states. Among those states resolved were the 87 keV, 233 keV, and 995 keV states in ^{69}Ge , which are populated by $\ell=1$ transitions and have assigned spin-parities of $1/2^-$, $3/2^-$ and "unknown" respectively. The angular distributions for these states are shown in Figure 8. The characteristic shapes of the known $2p_{1/2}$ and $2p_{3/2}$ transitions are consistent with the results of the $^{60}\text{Ni}(p,d)$ reaction and indicate an assignment of $1/2^-$ for the 995 keV state.

1159 keV state: This state, as all states of higher excitation energy populated by an $\ell=1$ transition, is assumed

Figure 8. Experimental angular distributions for three states observed in the $^{70}\text{Ge}(p,d)$ reaction at 25 MeV showing the $\ell=1$ j-dependence. The solid curves are drawn through the points to guide the eye.

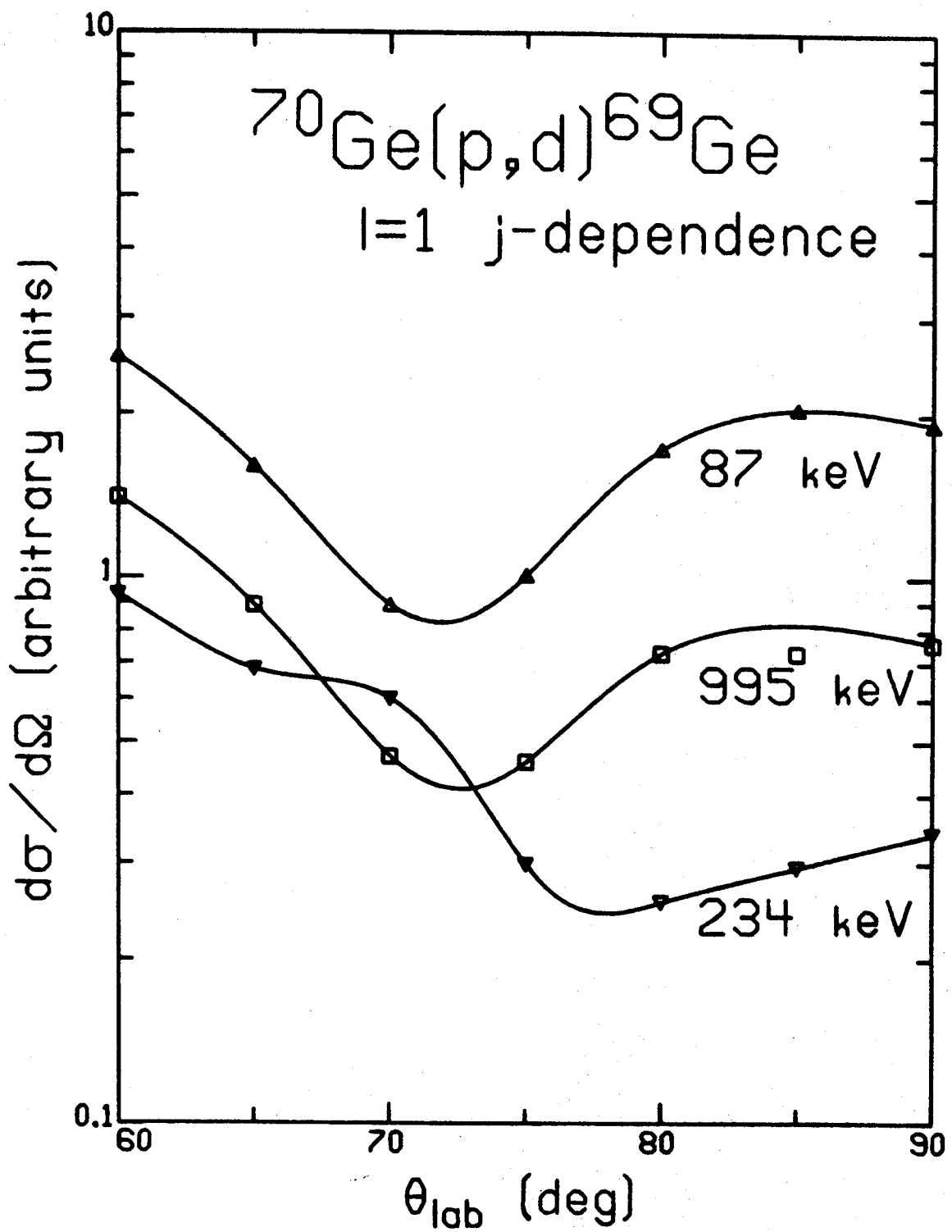


Figure 8

to have a spin-parity of $3/2(1/2)^-$. The preference for $3/2^-$ is based on the fact that we would expect less $2p_{1/2}$ strength with this target than with the others and the 87 keV and 995 keV states carry almost as much $2p_{1/2}$ strength as is seen in the $^{72}\text{Ge}(p,d)$ reaction. Of course, since this state (and several higher excited states) has a fairly small spectroscopic factor, this is not conclusive evidence. For those states with larger $\ell=1$ strengths (i.e. the 2106 keV state with $S=.16$) the $1/2^-$ possibility is less likely.

1468 keV and 1477 keV states: Our data show that these states are populated by $\ell=4$ and $\ell=3$ transitions respectively. Hsu et al.¹⁷⁾ were unable to fit the angular distribution for the 1477 keV state, but undoubtedly did not resolve the 1468 keV state. Both an $\ell=3$ and an $\ell=4$ shape are shown with the data in reference 17 and it appears that an $\ell=3+4$ mixture would do a satisfactory job of reproducing the experimental shape as observed there.

2985 keV and 3460 keV states: These states are weakly populated and the resulting poor statistics do not allow us to distinguish well between ℓ -transfers. Therefore, the ℓ -value assignments for these transitions are tentative on the basis of our data.

V. THE $^{72}\text{Ge}(p,d)^{71}\text{Ge}$ REACTION

V.1 General Comments

The results of this reaction are summarized in Table 3 and the angular distributions are shown in Figures 9 and 10. The second plate for this reaction showed no peaks stronger than 20 $\mu\text{b}/\text{sr}$ at 6° between 4.5 MeV and 8 MeV excitation. We find excellent agreement between the excitation energies determined in the present work and those from γ -ray experiments. Up through the 1743 keV state, which is the highest excited state with which we can make comparisons, the agreement is within 1 keV. In general the ℓ -values and spectroscopic factors obtained in the present study are in agreement with the previous (p,d) results of Fournier et al.¹⁸⁾ The main differences are that our $\ell=1$ spectroscopic factors are all about 20% lower than the previous work and our improved resolution allows us to correct some ℓ -value assignments. It is difficult to make comparisons with the (d,p) results beyond the lowest lying states, where we find agreement in ℓ -values. For the higher excited states, the (d,p) reaction sees many states populated by $\ell=2$ transitions while the (p,d) reaction shows almost none, presumably because the $2d_{5/2}$ orbit, as well as the $2d_{3/2}$ is almost empty.

The pattern of the $1/2^-$ and $3/2^-$ states may be broken in this nucleus as the (p,d) reaction populates no state near 1 MeV with a definite $1/2^-$ spin assignment. Malan et al.⁶⁾

Table 3. Summary of results for states in ^{71}Ge .

E_x (keV)	$^{72}\text{Ge}(p,d)$ Present Work		$^{72}\text{Ge}(p,d)$ Fournier et al. (18)		$^{70}\text{Ge}(d,p)$ Goldman (13)		Yray Malan et al. (5,6) & Murray et al. (9)		E_x (keV) c)	Combined Results for ^{71}Ge (6)	J^π
	ℓ	C^2S	ℓ	C^2S	ℓ	$(2J+1)S$	J^π	J^π			
0	1	.86	1	1.04	1	.55	1/2 ⁻	1/2 ⁻	0 (60±10)		1/2 ⁻
174	3	3.72	3	3.64	3	weak	5/2 ⁻	5/2 ⁻	174.9		5/2 ⁻
198	4	1.97	4	1.93	4	7.3	9/2 ⁺	9/2 ⁺	198.3		9/2 ⁺
500	1	1.61	1	2.32	1	.27	3/2 ⁻	3/2 ⁻	500.0		3/2 ⁻
524	2	.18			2	.62	5/2 ⁺	5/2 ⁺	524.1		5/2 ⁺
						weak		7/2(9/2)	589.2		7/2(9/2)
						weak			620±15		
						weak			630±15		
708	1	.14	1	.17	(1)	.054	3/2 ⁻	3/2 ⁻	708.2		3/2 ⁻
747	3	.38	3	.31	(2)	.021	5/2 ⁻	3/2, 5/2 ⁻	747.2		5/2 ⁻
(807)						weak			790±15		
831	1	.01	2	.03	(1)	.014	5/2 ⁺	1/2 ⁻	808.1		1/2 ⁻
						weak		3/2 ⁺	831.2		3/2 ⁻
						(1)			890±15		
						weak			950±15		
						weak			970±15		
1026	3	.16	2	.03			5/2 ⁻	5/2 ⁻ (5/2 ⁺)	1026.6		5/2 ⁻
						weak		9/2 ⁺ (9/2 ⁻)	1037.5		9/2 ⁺ (9/2 ⁻)
1095	1	.29	1	.37	1	.1	3/2 ⁻	3/2 ⁻	1095.6		3/2 ⁻

Table 3 - Continued.

E_x (keV)	$^{72}\text{Ge}(p,d)$ Present Work		$^{72}\text{Ge}(p,d)$ Fournier et al. 18)		$^{70}\text{Ge}(d,p)$ Goldman 13)		γ -ray Malan et al. 5,6) & Murray et al. 9)		Combined Results for ^{71}Ge 6)	
	ℓ	C^2S	ℓ	C^2S	ℓ	$(2J+1)S$	J^π	J^π	E_x (keV)	J^π
(1169)			1	.05	3/2(1/2) ⁻	weak	3/2	3/2	1139.4	3/2
1207*	3	.19	3	.40	5/2 ⁻	2? .029	5/2 ⁺ , 3/2 ⁺ (7/2)	5.2 ⁻	1167±5	5.2 ⁻
1288	1	.12	1	.18	3/2 ⁻	2? .039	1/2, 3/2, 5/2 ⁻	1/2, 3/2, 5/2 ⁻	1204.5	1/2, 3/2, 5/2 ⁻
1349	0	.01	2	.03	5/2 ⁺	weak	3/2 ⁻ , 1/2 ⁻	1288.3	1288.3	3/2(1/2) ⁻
1379						0 .093	1/2, 3/2, 5/2	1298.7	1348.8	1/2 ⁺
1408*	3	.14	3	.26	5/2 ⁻	(2) .09	(1/2 ⁻), 3/2 ⁺ , (3/2 ⁻)	1378.9	1378.9	3/2(1/2) ⁻
						weak	1/2 ⁻ , 3/2, 5/2 ⁻	1407.0	1407.0	
						weak		1414.5	1414.5	
						weak		1454.2	1454.2	
1506	3	.40	3	.53	5/2 ⁻	(3) .55 (5/2 ⁻)	5/2, 7/2	1476.5	1476.5	5/2 ⁻ (7/2)
1558	3	.07				(2) .057	1/2, 3/2, 5/2	1506.6	1506.6	5/2 ⁻
1598	1	.04	1	.09	3/2(1/2) ⁻	2 .21		1543.0	1543.0	5/2 ⁻
								(1565.5)	(1565.5)	
1743	1	.04	1	.09	3/2(1/2) ⁻	(3) .63	3/2(1/2) ⁻	1599.0	1599.0	3/2(1/2) ⁻
							1/2, 3/2, 5/2 ⁻	1629.4	1629.4	1/2, 3/2, 5/2 ⁻
							(1/2), 3/2, 5/2	1698.6	1698.6	(5/2 ⁻)
								1743.5	1743.5	3/2(1/2) ⁻

Table 3 - Continued.

E_x (keV)	$^{72}\text{Ge}(p,d)$ Present Work		$^{72}\text{Ge}(p,d)$ Fournier et al. 18)		$^{70}\text{Ge}(d,p)$ Goldman 13)	γ -ray Malan et al. 5,6) & Murray et al. 9)		Combined Results for ^{71}Ge 6)			
	λ	C^2S	J^π	λ		C^2S	J^π	J^π	E_x (keV) c)	J^π	
1780	3	.23	5/2 ⁻	3	.42	5/2 ⁻	(1)	.013	(3/2 ⁻)	1792.7	5/2 ⁻
								weak		1870 \pm 15	
1963	1	.11	3/2(1/2) ⁻	1	.18	3/2(1/2) ⁻	0	weak	1/2 ⁻ , 3/2, 5/2 ⁻	1938.2	
1979 ^{a)}								.039	1/2 ⁺	1965.4*	1/2 ⁺ +3/2 ⁻ (1/2 ⁻)
2031	1	.02	3/3(1/2) ⁻				1	.097	3/2 ⁻	1979 \pm 5	3/2(1/2) ⁻
2045 ^{a)}										2031 \pm 5	
										2045 \pm 5	(5/2 ⁻)
2221	0	.02	1/2 ⁺				(3)	.12	(5/2 ⁻)	2120 \pm 15	
2241 ^{a)}								weak		2170 \pm 15	
2256 ^{a)}							0	.25	1/2 ⁺	2221 \pm 7	1/2 ⁺
										2241 \pm 5	
										2256 \pm 5	
2279 ^{a)}	1	.03	3/2(1/2) ⁻				2	.27		2270 \pm 15	(5/2 ⁺)
										2279 \pm 5	3/2(1/2) ⁻
2348	1	.10	3/2(1/2) ⁻	1	.18	3/2(1/2) ⁻		weak		2330 \pm 15	3/2(1/2) ⁻
2384 ^{a)}	3	.14	5/2 ⁻				0	.02	1/2 ⁺	2348 \pm 5	5/2 ⁻
										2384 \pm 7	1/2 ⁺
2479 ^{a)}										2410 \pm 15	
2487	0	.01	1/2 ⁺				0	.044	1/2 ⁺	2479 \pm 10	1/2 ⁺
										2487 \pm 10	

Table 3 - Continued.

E_x (keV)	$^{72}\text{Ge}(p,d)$ Present Work		$^{72}\text{Ge}(p,d)$ Fournier et al. 18)		$^{70}\text{Ge}(d,p)$ Goldman 13)		γ -ray Malan et al. 5,6) & Murray et al. 9)		Combined Results for ^{71}Ge 6)	
	λ	C^2S	J^π	λ	C^2S	J^π	λ	J^π	E_x (keV) c)	J^π
2675 ^a)	1	.03	$3/2(1/2)^-$						2675 \pm 5	$3/2(1/2)^-$
2697 ^a)									2697 \pm 7	
2709 ^a)	4	.09	$9/2^+$						2709 \pm 5	$9/2^+$
2778 ^a)	1	.02	$3/2(1/2)^-$						2778 \pm 7	$3/2(1/2)^-$
2865 ^a)	0	.03	$1/2^+$						2865 \pm 5	$1/2^+$
2889 ^a)	1	.02	$3/2(1/2)^-$						2889 \pm 10	$3/2(1/2)^-$
2913 ^a)	2	.02	$5/2^+$						2913 \pm 10	$5/2^+$
2950 ^a)									2950 \pm 10	
3100 ^a)									3100 \pm 5	
3195 ^a)									3195 \pm 10	
3217 ^a)									3217 \pm 10	
3232 ^a)									3232 \pm 10	
3263 ^a)									3263 \pm 10	
3287 ^a)	1	.07	$3/2(1/2)^-$						3287 \pm 7	$3/2(1/2)^-$
3369 ^a)	1	.02	$3/2(1/2)^-$						3369 \pm 7	$3/2(1/2)^-$
3518 ^a)	1	.01	$3/2(1/2)^-$						3518 \pm 7	$3/2(1/2)^-$
3533 ^a)									3533 \pm 7	
3556 ^a)									3556 \pm 7	
3568 ^a)									3568 \pm 10	
3667 ^a)									3667 \pm 7	

Table 3 - Continued

E_x (keV)	$^{72}\text{Ge}(p,d)$ Present Work		$^{72}\text{Ge}(p,d)$ Fournier et al. 18)		$^{70}\text{Ge}(d,p)$ Goldman 13)		γ -ray Malan et al. 5,6) & Murray et al. 9)		Combined Results for ^{71}Ge 6)	
	λ	C^2S	J^π	C^2S	J^π	λ	$(2J+1)S$	J^π		E_x (keV) c)
3677 ^{a)}									3677 \pm 7	
3769 ^{a)}	3	.11	$5/2^-$						3769 \pm 7	$5/2^-$
3790 ^{a)}	1	.12	$3/2(1/2)^-$						3790 \pm 10	$3/2(1/2)^-$
3900 ^{a)}	1	.02	$3/2(1/2)^-$						3900 \pm 10	$3/2(1/2)^-$
3932 ^{a)}	1	.02	$3/2(1/2)^-$						3932 \pm 10	$3/2(1/2)^-$
3961 ^{a)}									3961 \pm 10	
3986 ^{a)}									3986 \pm 10	
4066 ^{a)}									4066 \pm 10	
4230 ^{a)}									4230 \pm 10	
4388 ^{a)}									4388 \pm 10	

* Doublet.

a) States seen for the first time in the present work.

b) Compiled from the results of the present work and those of References 5,6,9,10, and 14.

c) Uncertainties are ± 1 keV for energies quoted to a tenth of a keV.

Figure 9. Experimental angular distributions obtained from the $^{72}\text{Ge}(p,d)$ reaction at 35 MeV. The solid curves are fits to the data of DWBA predictions.

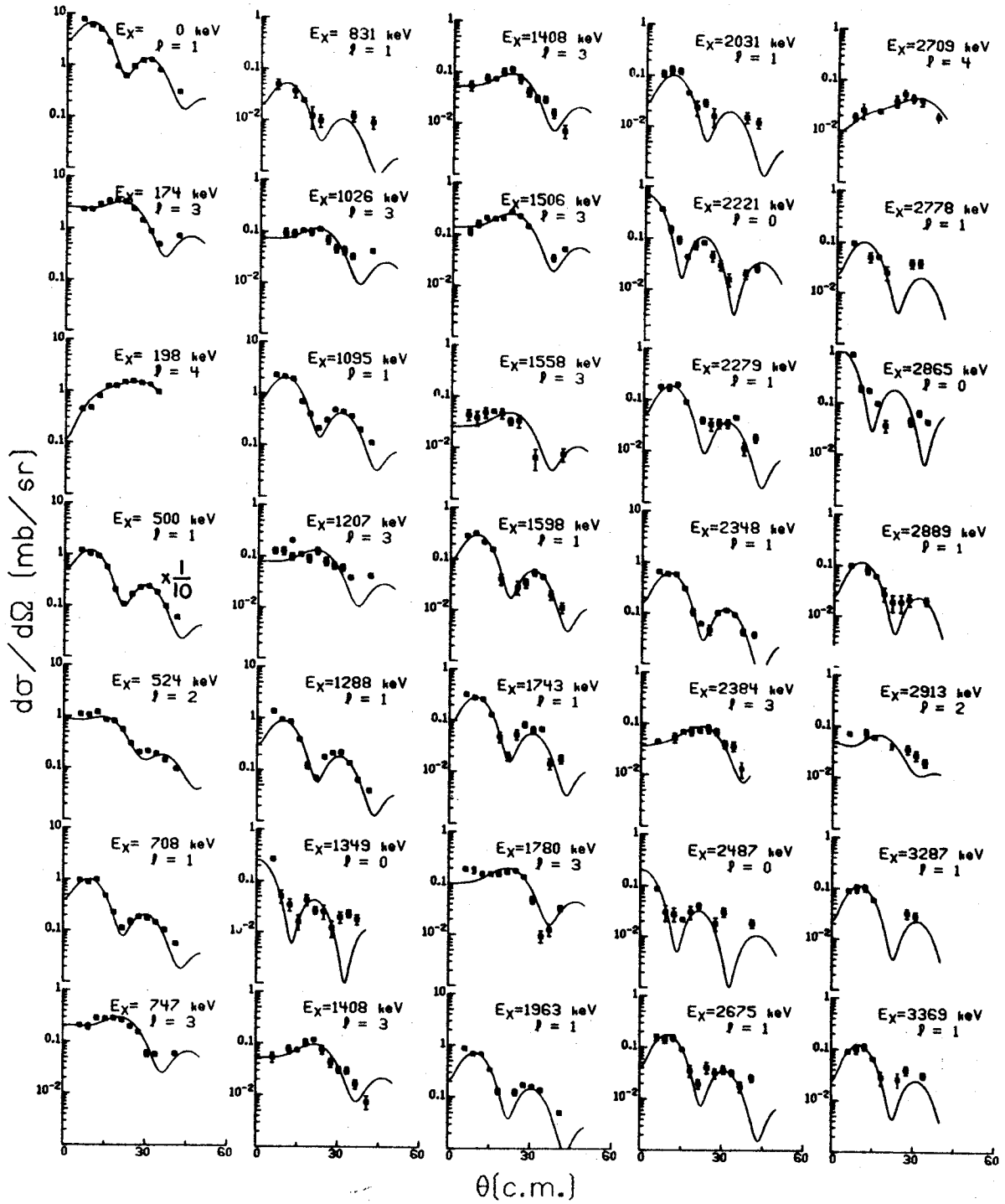


Figure 9

rom
curves

Figure 10. Experimental angular distributions obtained from the $^{72}\text{Ge}(p,d)$ reaction at 35 MeV. The solid curves are fits to the data of DWBA predictions.

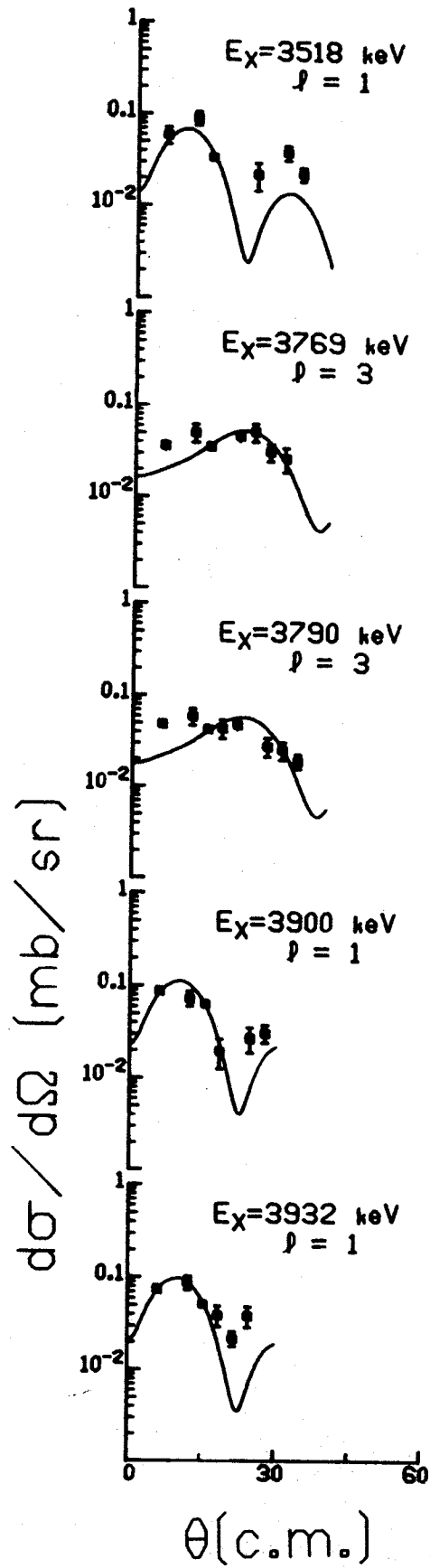


Figure 10

have assigned a spin of $1/2^-$ to the 1289 keV state, which we observe, but the assignment is based on excitation intensities which are not conclusive in this case. Since the other possible candidates for the $1/2^-$ state in this region (i.e. the 708 keV and 1095 keV states) have been confirmed to be $3/2^-$ states, the $\ell=1$ systematics support the $1/2^-$ assignment for the 1289 keV state. However, we do not consider this spin to be firmly established.

Another feature of the distribution of $\ell=3$ strength, which shows up most clearly in this nucleus, is the presence of a weak $\ell=3$ transition to a state near 3.7 MeV. This state follows a gap of almost 1 MeV in which there are no states populated by an $\ell=3$ transfer. It might be inferred that these states near 3.7 MeV are $7/2^-$ states but there is no other evidence to support such an idea.

V.2 Comments on Individual States

500 keV state: This state is strongly populated in the (p,d) reaction by an $\ell=1$ transfer. The ratio of (p,d) strength to (d,p) strength suggests a $3/2^-$ spin assignment for this state and this is the only state in this nucleus to match the strongly populated $3/2^-$ states seen in the other odd nuclei. These considerations are in agreement with the $3/2^-$ spin assignment of Murray et al.⁹⁾ Goldman,¹⁴⁾ in disagreement with the above results, assigns a spin of $1/2^-$ to this state based on the Lee-Schiffer effect. This discrepancy in $\ell=1$ spin assignments is also seen in a few of the higher

excited states. Fournier et al.¹⁸⁾ have suggested that Goldman's data do not convincingly display the Lee-Schiffer effect at 140° as claimed, since only one $\ell=1$ angular distribution (for the 2040 keV state) really does not show a dip here. This observation, coupled with poor statistics shown in the (d,p) data, makes it doubtful that spin assignments can be made from this data. It would be interesting to look for the $\ell=1$ J-dependence in the germanium isotopes with high resolution and good statistics with both the (p,d) and (d,p) reactions to help clarify the situation.

807 keV state: While this state has been observed in γ -ray work, we see only a very weak (≤ 0.015 mb/sr at 6°) peak at this energy. Fournier et al.¹⁸⁾ report an $\ell=2$ transition to a state at this energy, but this is in disagreement with the $1/2, 3/2$ spin assignment from the γ -ray work. The $\ell=2$ transition shown in Reference 18 is probably the sum of the 831 keV $\ell=1$ transition and the $^{70}\text{Ge}(p,d)$ $\ell=3$ transition to the ground state of ^{69}Ge . These two states would not have been resolved in the previous (p,d) experiment. This would then remove the conflict with the γ -ray results.

831 keV state: We observe a weak but distinct $\ell=1$ transition to this state which implies a spin of $1/2^-$ or $3/2^-$. The negative parity is in disagreement with the results of Malan et al.⁶⁾ which indicate a spin of $3/2^+$ for this state. There is no evidence for a doublet at this energy, and our energy calibration is in close agreement with the γ -ray work

so that we can put an upper limit of 1 keV for the separation of the two states if there is a doublet here. The positive parity assignment is based on the excitation intensity at one bombarding energy only. Also, the γ -ray angular distribution for the decay to the ground state favors a significant M2/E1 mixing ratio which is unlikely. We therefore favor the $3/2^-$ spin assignment for this state.

1026 keV state: This state is weakly populated in the (p,d) reaction which makes it difficult to make a definite ℓ -transfer assignment. However, our angular distribution for this state is sufficiently distinct to establish that this state is populated by an $\ell=3$ transition, which is in agreement with the $3/2, 5/2^-$ spin assignment of Malan et al.⁶⁾ Fournier et al.¹⁸⁾ report at $\ell=2$ transition to this state, but would not have resolved the $^{70}\text{Ge}(p,d)$ $\ell=1$ transition to the 234 keV state in ^{69}Ge . This fact, coupled with their poor statistics, probably accounts for their $\ell=2$ assignment.

1169 keV state: This state is very weakly populated in our data and is almost obscured (<15 keV separation) by the stronger $^{70}\text{Ge}(p,d)$ $\ell=1$ transition to the 374 keV state in ^{69}Ge . Fournier et al.¹⁸⁾ report on $\ell=1$ transition to a state at 1166 keV but most likely it is the impurity which is being seen and not a state in ^{71}Ge .

1207 keV doublet: Examination of the spectra indicate that there is a doublet at this energy of about 7 keV which we do not completely resolve. The states are weakly

populated which makes it impossible to separate the peaks by a fitting procedure and also makes it difficult to determine the ℓ -transfers for the states. The $\ell=3$ fit to the summed angular distribution is sufficiently good that we could not justify adding in another component, although an $\ell=2+3$ mixture would fit the data slightly better. An $\ell=2+3$ mixture would be in agreement with Goldman's data¹⁴⁾ as the (d,p) angular distribution appears to be predominately an $\ell=2$ shape but would be better fit by an $\ell=2+3$ mixture. The $\ell=2+3$ mixture would also fit in well with the results of Malan et al.⁶ as the higher member of the doublet has been assigned a spin of $5/2^-$ and the lower member has $5/2^+$ as one of the possible spins.

1506 keV and 1558 keV states: Our data show distinct $\ell=3$ transitions to both of these states even though the 1558 keV state is weakly populated. Goldman¹⁴⁾ has assigned tentative $\ell=2$ transfers for these states but the (d,p) data exhibit poor statistics. Also, the (d,p) angular distribution for the 1558 keV state is quite similar to the (d,p) $\ell=3$ angular distributions. It therefore appears that the $\ell=2(?)$ assignments are incorrect and these states are indeed populated by $\ell=3$ transitions.

1963 keV state: The (p,d) angular distribution for this state shows a definite $\ell=1$ shape while the (d,p) angular distribution shown by Goldman¹⁴⁾ shows a definite $\ell=0$ shape. It therefore appears that the (p,d) and (d,p) reactions are populating different states. It is not surprising that the

(p,d) reaction does not strongly populate a $1/2^+$ state here, even if it exists, since we do not expect any significant filling of the $3s_{1/2}$ orbit in the ground state of ^{72}Ge .

2279 keV state: Again this state is probably not the same as Goldman's¹⁴⁾ 2270 keV state as the (d,p) angular distribution is definitely not compatible with the $\ell=1$ transition shown in our (p,d) data. Our angular distribution does show some filling in of the first minimum which could be an indication of an $\ell=2$ or an $\ell=3$ component, but there is no other evidence in our data for a doublet. In particular, if there were two states separated by more than 7 keV we should observe a broadening of the peak in the spectrum. It is therefore likely that either the (d,p) data is incorrect or the (p,d) reaction does not populate the 2270 keV state.

Beyond this point it is impossible to make associations between those states seen in our data and those reported by Goldman.¹⁴⁾

VI. THE $^{73}\text{Ge}(p,d)^{72}\text{Ge}$ REACTION

VI.1 General Comments

In this reaction, the nonzero spin of the target nucleus allows more than one ℓ -transfer to populate a given state. In particular, we expect to see many states populated by an $\ell=1+3$ mixture and a few by an $\ell=2+4$ mixture. This is indeed the case as is shown in the summary of results for this reaction in Table 4 and in the angular distributions shown in Figures 11 and 12. The excitation energies, ℓ -values, and spectroscopic factors obtained in the present study are in general in good agreement with the results of previous work. We again observe many states and their characteristics about which nothing was previously known. The second plate showed no peaks stronger than 25 $\mu\text{b}/\text{sr}$ at 6° between 5.8 MeV and 10 MeV excitation.

Where mixed ℓ -transfers are allowed, the extracted spectroscopic factors must have a larger uncertainty associated with them. In particular, the strength of an $\ell=3$ component mixed in with a predominately $\ell=1$ transition is determined entirely by the filling in of the first minimum of the $\ell=1$ shape. The quality and quantity of our data do not allow us to determine this filling exactly. This uncertainty undoubtedly accounts for the fact that our summed $\ell=3$ strength for this nucleus exceeds the sum-rule limit while it does not exceed the limit for any of the other isotopes.

Table 4. Summary of results for states in ^{72}Ge

E_x (keV)	$^{73}\text{Ge}(p,d)$ Present Work		$^{73}\text{Ge}(p,d)$ Fournier et al. ¹⁸⁾		$^{73}\text{Ge}(p,d)$ Rester ²⁾		^{73}Ge Camp ¹³⁾		Combined Results for ^{72}Ge ^{b)}	
	ℓ	C^2S	ℓ	C^2S	J^π	J^π	J^π	J^π	E_x (keV) ^{c)}	J^π
0	4	.58	4	.52	0^+	0^+	0^+	0	0^+	
691		.01		.003	0^+	0^+	0^+	691.2	0^+	
834	2	.05	2	.04	2^+	2^+	2^+	834.0	2^+	
1463	2	.19	2	.01	2^+	2^+	2^+	1463.9	2^+	
1728	4	.28	4	.23	4^+	4^+	4^+	1728.2	4^+	
2065	2	.01	2	.01	$3(+)$	$3(+)$	3^+	2064.8	3^+	
2402	2	.01			(2^+)	(2^+)	(2^+)	2402.0	(2^+)	
2464	2	.02			$(3^+, 4^+)$	$(3^+, 4^+)$	(4^+)	2463.7	$(3^+, 4^+)$	
2516	1	.26	1	.19	3^-	3^-	3^-	2514.7	3^-	
			4	.19						
2757	4	.05	1	.05	$(1, 2)$	$(1, 2)$	$(1, 2)^+$	(2583.5)	$(1, 2)$	
2774 ^{a)}	2	.02			$(1-3)^+$	$(1-3)^+$		2754.1	$(1-3)^+$	
	4	.04						2774 \pm 5		
2943	3	.08	3	.11	(3^-)	(3^-)	(1^-)	2939.7	(1^-)	
2952	4	.07					(3^-)	2943.4	(3^-)	
								2950.3		

Table 4 - Continued.

E_x (keV)	$^{73}\text{Ge}(p,d)$ Present Work		$^{73}\text{Ge}(p,d)$ Fournier et al. 18)		$^{73}\text{Ge}(p,d)$ Rester ²⁾		^{73}Ge Camp ¹³⁾		Combined Results for $^{72}\text{Ge}^{b)}$	
	λ	C^2S	λ	C^2S	J^π	J^π	J^π	J^π	E_x (keV) ^{c)}	J^π
3036	2 4	.01 .10	3	.22	(2 ⁻)		2 ⁻		3035.5	(2 ⁻)
3075	2 4	.01 .15		weak					3075±5	
3098	2	.01			(1 ⁺ , 2 ⁺)		(2 ⁺)		3093.8	2 ⁺
3131	1 3	.08 .06	1	.06					3131±5	
3250	1	.06	1	.06					3250±5	
3327	1	.12	1	.09	3 ⁻		3 ⁻		3324.9	3 ⁻
							(1, 2 ⁺)		3338.1	(1, 2 ⁺)
					2 ⁻		2 ⁻		3341.6	2 ⁻
3405	1 3	.39 .29	1+3 1+4	.28, .50 .28, .60					3405±5	
							(1 ⁻)		3419.4	(1 ⁻)
					(2 ⁺ , 3, 4 ⁺)		(4 ⁻)		3439.3	(2 ⁻)
					(2, 3, 4 ⁺)		(2 ⁻)		3455.2	(1 ⁻)
							(1 ⁻)		3550.3	(3 ⁻ , 4 ⁻)
3568	1	.10	1	.07	(2-4)				3566.0	
3588 ^{a)}	3	.06	3	.18					3588±5	

Table 4 - Continued.

E_x (keV)	^{73}Ge (p,d) Present Work		^{73}Ge (p,d) Fournier et al. ¹⁸		γ -ray Rester ²⁾ J^π	γ -ray Camp ¹³⁾ J^π	Combined Results for ^{72}Ge (b)	
	ℓ	C^2S	ℓ	C^2S			E_x (keV) (c)	J^π
3627	1 3	.01 .06					3619.5	
3658	1 3	.17 1.0	1+3 1+4	.32, 1.28 .32, 1.41			3658±5	
3668	1 3	.2 .32					3667.2	
3681	1 3	.17 .21			(2 ⁻ , 3 ⁻)		3678.1	3 ⁻
3702							3707.1	(2-4)
3762	1 3	.19 1.36	1+3 1+4	.38, .9 .36, 1.14	(3 ⁻ , 4 ⁻)		3758.6	(3 ⁻ , 4 ⁻)
3822	1	.32				(1 ⁻)	3803.1	(1 ⁻)
3867 ^{a)}	2	.03				(3 ⁻)	3815.2	3 ⁻
3880	1 3	.02 .22	3	1.23			3867±7	
3902 ^{a)}	3	1.17					3880±7	
3920	2	.06					3902±7	
3942 ^{a)}							3920±10	
							3942±10	

Table 4 - Continued.

E_x (keV)	$^{73}\text{Ge}(p,d)$ Present Work		$^{73}\text{Ge}(p,d)$ Fournier et al. 18)		γ -ray Rester. 2) J^π	γ -ray Camp 13) J^π	Combined Results for $^{72}\text{Ge}^b$ E_x (keV c)	J^π
	ℓ	C^2S	ℓ	C^2S				
3986	1 3	.11 .19	1 3	.15 .50		(2, 3 $^-$)	3983.7	3 $^-$
4016 ^{a)}						(1 $^-$)	(3985.0) 3995.3	(1 $^-$)
4040	1 3	.09 .12				(3, 2 $^-$)	4016 \pm 10 4041.2	3 $^-$
4056	1 3	.08 .12	1 3	.24 .53			4056 \pm 7	
4076 ^{a)}	1 3	.16 .27					4076 \pm 7	
4207	1	.3	1	.27		(1 $^-$)	4090.3	(1 $^-$)
4230 ^{a)}	(0)						4207 \pm 7	
4282 ^{a)}	2	.03					4230 \pm 7 4282 \pm 7	(4 $^+$, 5 $^+$)
4335	1	.04	1+3 1+4	.37, .51 .37, .51			4335 \pm 7	
4354 ^{a)}	1	.32					4354 \pm 7	
4379 ^{a)}	1	.06					4379 \pm 7	

Table 4 - Continued

E_x (keV)	$^{73}\text{Ge}(p,d)$ Present Work		$^{73}\text{Ge}(p,d)$ Fournier et al. 18)		γ -ray Rester ²⁾		γ -ray Camp ¹³⁾		Combined Results for ^{72}Ge b)	
	λ	C^2S	λ	C^2S	J^π	J^π	J^π	J^π	E_x (keV) c)	J^π
5099 ^{a)}	3	.09							5099 \pm 7	
5164 ^{a)}	0	.00							5164 \pm 7	(4 ⁺ , 5 ⁺)
5192 ^{a)}	2	.01							5192 \pm 7	
5234 ^{a)}	1	.01							5234 \pm 7	
5312 ^{a)}	1	.01							5312 \pm 7	
5312 ^{a)}	3	.03							5312 \pm 7	
5354 ^{a)}	1	.02							5354 \pm 7	
5408 ^{a)}	3	.06							5408 \pm 10	
5438 ^{a)}	3	.08							5438 \pm 10	
5563 ^{a)}									5563 \pm 10	
5650 ^{a)}	1	.02							5650 \pm 10	

* Doublet.

a) Seen for the first time in the present work.

b) Compiled from the results of the present work and those of references 2, 12, and 13.

c) Uncertainties are ± 1 keV for energies quoted to tenth keV accuracy.

Figure 11. Experimental angular distributions obtained from the $^{73}\text{Ge}(p,d)$ reaction at 35 MeV. The solid curves are fits to the data of DWBA predictions. For mixed ℓ -transfers, the dashed lines show the contribution of each component.

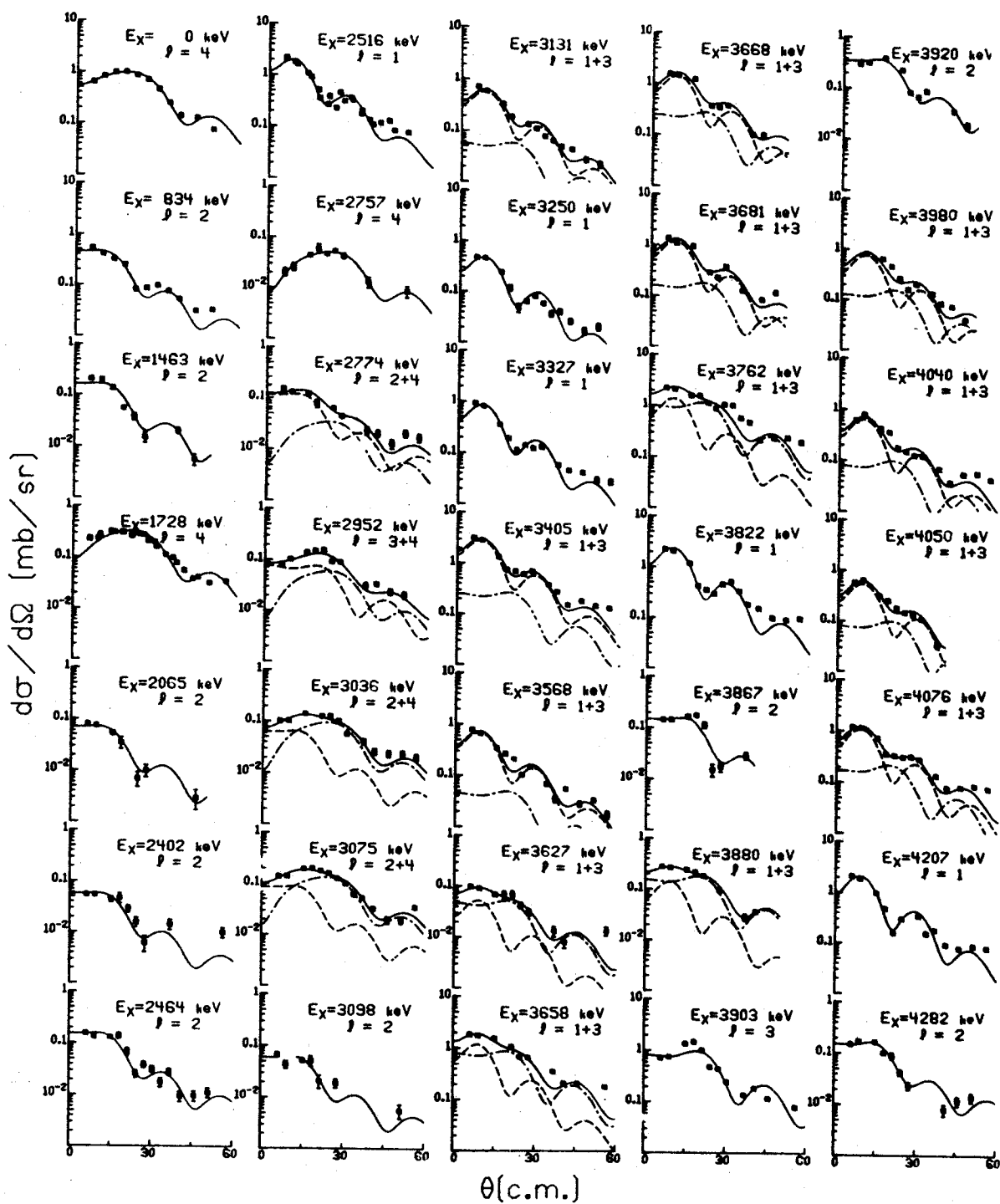


Figure 11

Figure 12. Experimental angular distributions obtained from the $^{73}\text{Ge}(p,d)$ reaction at 35 MeV. The solid curves are fits to the data of DWBA predictions. For mixed ℓ -transfers, the dashed lines show the contribution of each component.

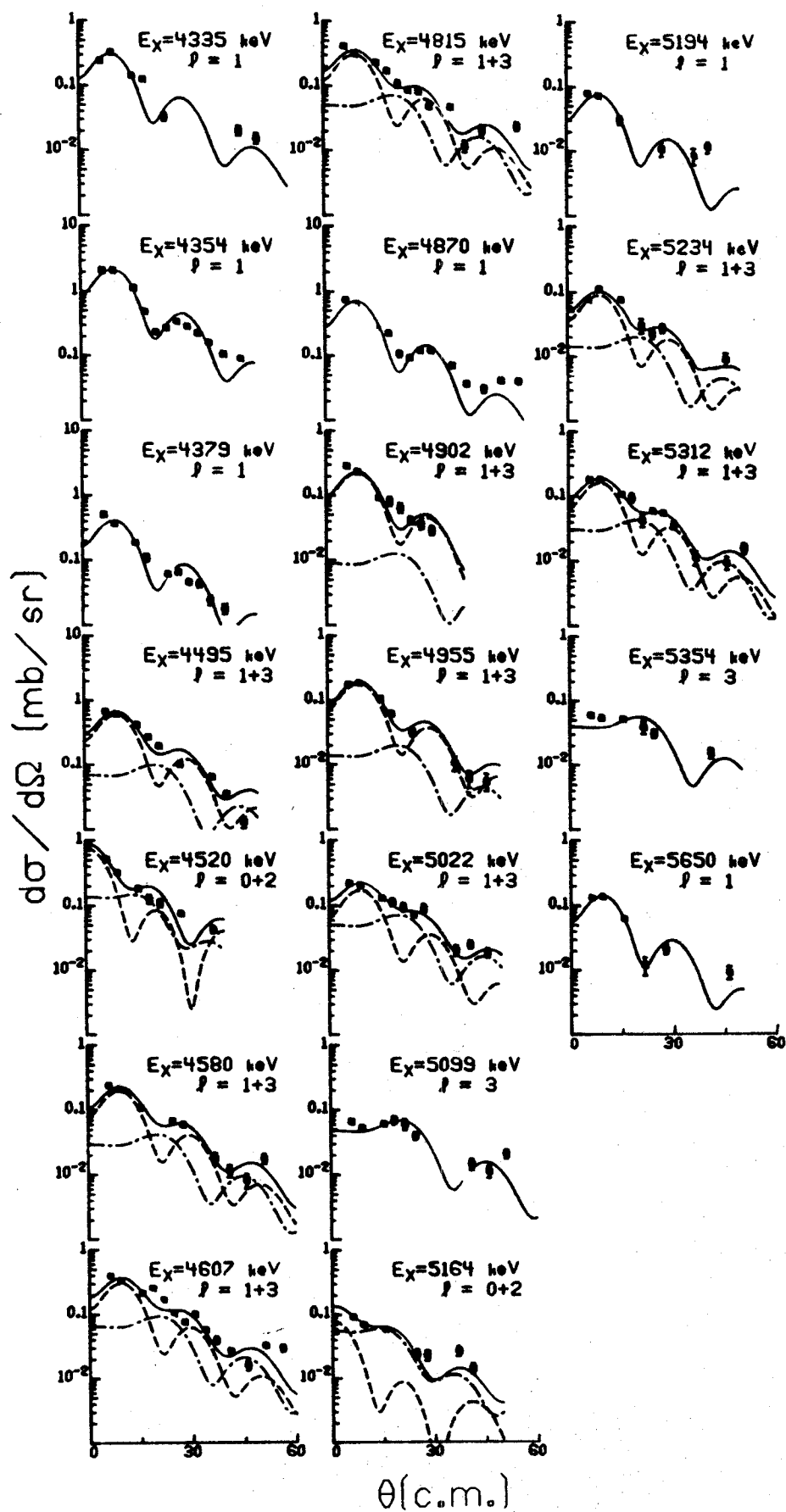


Figure 12

from
ons.
the

VI.2 Comments on Individual States

2464 keV and 2516 keV states: Our data show a weak $\ell=2$ and a strong $\ell=1$ transition to these states respectively. These are both in agreement with the spins and parities previously reported for these states. Fournier et al.¹⁸⁾ do not report the 2404 keV state, but probably did not resolve it from the 2516 keV state. The angular distribution shown in Reference 18 is therefore probably the sum of these two transitions. Fournier et al. fit the distribution with an $\ell=1+4$ mixture, but it appears that an $\ell=1+2$ mixture would fit the data satisfactorily. We see no evidence in our data for an $\ell=4$ component to either transition.

2757 keV state: We observe a distinct, although weak, $\ell=4$ transition to this state which is in agreement with the $(1-3)^+$ spin assignment of Rester et al.²⁾ Fournier et al.¹⁸⁾ report a stronger $\ell=1$ transition to this state which is not only in disagreement with our data, but also implies a negative parity in contradiction to the γ -ray work. However, the $\ell=1$ assignment is based primarily on only two data points at about 15° . It is possible that in the previous (p,d) work this state was not adequately resolved at these two angles from the $^{13}\text{C}(p,d)$ transition to the 4.4 MeV state in ^{12}C .

2943 keV and 2952 keV states: These states are not completely resolved in most of our spectra, although there is a consistent broadening of the peak of about three channels in all the spectra. The sum of the angular distributions

is plotted in the figure under an excitation energy of 2952 keV. The spin and parity of the 2943 keV state allows an $\ell=1$ component in the transition to this state, and there could be an $\ell=2$ component in the transition to the 2952 keV state. However, we cannot determine the strengths of these transitions, or even if they exist, since the shape of the summed angular distribution is reproduced well by the $\ell=3+4$ mixture.

3036 keV state: The angular distribution that we obtain for this state does not allow us to distinguish well between an $\ell=2+4$ or an $\ell=3+4$ mixture, but the existence of the $\ell=4$ component is firmly established. The $\ell=3+4$ fit has a χ^2 of about one half that for the $\ell=2+4$ fit but both reproduce the shape well. Based on our data alone we would choose the $\ell=2+4$ mixture since this does not require the state to be a doublet. These are the results shown in the figure and table. Fournier et al.¹⁸⁾ report an $\ell=3$ transition to this state but it appears that the angular distribution shown in Reference 18 could be fitted well by either an $\ell=2+4$ or an $\ell=3+4$ mixture. The γ -ray results present a contradiction as they indicate a negative parity for this state in disagreement with the positive parity indicated by the $\ell=4$ component to the (p,d) transition. If neither the negative parity of the γ -ray work, nor the $\ell=4$ component of our work is incorrect, then the state must be a doublet. In such a case we might best fit the angular distribution with the $\ell=3+4$ mixture. This would yield spectroscopic factors of .12 and .10

for the $\ell=3$ and $\ell=4$ components respectively.

3098 keV state: This state is weakly populated in the (p,d) reaction and our angular distribution is only fairly distinct. It does, however, strongly favor an $\ell=2$ transition to this state. Rester et al.²⁾ have assigned a spin of $(1,2)^+$ and Camp has tentatively assigned a spin of 2^+ . The $\ell=2$ transfer rules out the $J=1$ possibility since the transferred spin of $5/2$ cannot couple to the target spin of $9/2$ to yield a final spin of less than 2. This then confirms the 2^+ spin assignment of Camp.¹³⁾

3405 keV, 3658 keV, and 3762 keV states: In our data the angular distributions for these states are fitted best by an $\ell=1+3$ mixture. An $\ell=1+4$ mixture cannot be completely ruled out, but it is much less likely as the spectra show no evidence for doublets at these energies.

3568 keV state: The $\ell=1$ component to transition to this state in conjunction with the γ -ray work allows us to restrict the spin for this state to 3^- , 4^- . The γ -ray work of Rester et al.²⁾ has restricted the spin to $(2-4)$. The $\ell=1$ transition rules out the $J=2$ possibility and implies negative parity.

3681 keV, 3822 keV, 3986 keV, and 4040 keV states: For each of these states we can assign a spin of 3^- . In each case the γ -ray work^{2,13)} has restricted the spin to 2 or 3 and in each case we observe an $\ell=1$ component to the transition to the state. The $\ell=1$ component rules out the $J=2$ possibility

and implies negative parity, thus establishing the spin of 3^- .

3803 keV state: In our spectra the peak for this state would be covered by the peak for the $^{74}\text{Ge}(p,d)$ $\ell=1$ transition to the 393 keV state in ^{73}Ge . Fournier et al.¹⁸⁾ report a state at 3804 keV, but it is likely that it is actually this impurity which is being observed.

4230 keV state: This state is very weakly populated in the (p,d) reaction and the angular distribution is indistinct. However, there appears to be a definite forward angle rise which would indicate an $\ell=0$ transition. If the state is indeed populated by an $\ell=0$ transition its spin would have to be 4^+ or 5^+ .

4335 keV state: Our angular distribution for this state is not complete, but we see no evidence for either an $\ell=3$ or an $\ell=4$ component to the transition. Fournier et al.¹⁸⁾ report on $\ell=1+3$ or an $\ell=1+4$ transition to this state, but the data shown in reference 18 is not conclusive either.

Fournier et al.¹⁸⁾ report an $\ell=1$ transition to a state at 4458 keV. Our data show that the peak for this state would be covered by the peak for the $^{72}\text{Ge}(p,d)$ $\ell=1$ transition to the 500 keV state in ^{71}Ge . It is, therefore, doubtful that there is a state in ^{72}Ge at 4458 keV.

Also, Fournier et al.¹⁸⁾ have suggested that the $\ell=4$ components observed in the transitions to the states at 3398 keV, 3659 keV, 3754 keV, 3804 keV, and 4339 keV might be due to the 6^+ or 8^+ states that should be populated by $1g_{9/2}$

pickup. Our spectra and angular distributions indicate that these $g=4$ components probably do not exist. We do observe $g=4$ transitions to the states at 2774 keV, 2950 keV, 3036 keV, and 3075 keV which could be populating these high spin states. However, our data do not contain sufficient information to determine the spins of these states.

VII. THE $^{74}\text{Ge}(p,d)^{73}\text{Ge}$ REACTION

VII.1 General Comments

The results for this reaction are summarized in Table 5 and the angular distributions are shown in Figures 13 and 14. The second plate showed no peaks stronger than $15 \mu\text{b}/\text{sr}$ at 6° between 4.8 MeV and 8.5 MeV excitation. In general there is good agreement between the excitation energies, ℓ -values, and spectroscopic factors obtained in the present study and those obtained in previous work. There are several states and their characteristics which we observe about which nothing was previously known.

There is a slight variation in the $\ell=1$ transfer systematics for this nucleus. The $3/2^-$ strength near 500 keV is split into two close states at 364 keV and 394 keV. There is a $1/2^-$ state at 895 keV to complete the pattern of a $2p_{1/2}$ transfer to a state near 1 MeV. There is an $\ell=1$ transition to a state at 1044 keV which has been assigned a spin of $3/2^-$. Although a $1/2^-$ assignment for this state might fit the systematics better, Fournier et al. and Kato have preferred a $3/2^-$ assignment.

VII.2 Comments on Individual States

392 keV state: It is difficult to determine the spin of this state, which is populated by an $\ell=1$ transition, but $3/2^-$ appears to be the best choice. The ratio of (p,d) strength

Table 5. Summary of results for states in ^{73}Ge .

E_x (keV)	$^{74}\text{Ge}(p,d)$ Present Work		$^{74}\text{Ge}(p,d)$ Fournier et al. ¹⁸⁾		$^{72}\text{Ge}(d,p)$ Kato, 16) Hasselgren ³⁾ Heyman et al. ¹⁵⁾		Combined Results for ^{73}Ge b)	
	λ	J^π	λ	C^2S	λ	C^2S	λ	J^π
0	4	3.39	4	3.35	4	5.04	0	$9/2^+$
13	2	$.23$	2	$.21$	2	$.30$	(2.9)	$5/2^+, 1/2^+, 9/2^+$
66	1	$.59$	1	$.56$	1	$.52$	13.5	$5/2^+$
							66.7	$1/2^-$
353	3	2.94	3	2.58			68.7	$(7/2^+)$
364	1	1.14	1	2.03	1	$.48$	319.7	$5/2^-$
392	1	$.96$	1	2.03	1	$.65$	352.6	$5/2^-$
500	2	$.18$	2	$.08$ $.12$	1		363.3	$3/2(1/2)^-$
					2		391.7	$1/2^-(3/2^-)$
554	0	$.02$	2	$.06$	0	$.11$	499.1	$5/2^+$
598	3	$.12$					523.6	$1/2^+$
778	2	$.01$			3(4)	1.06	553.7	$5/2^-$
809	3	$.11$				weak	597.8	$5/2^-$
827						weak	655 ± 5	$5/2^+$
895	1	$.11$	1	$.19$	1	$.24$	778 ± 2	$5/2^-$
911	2	$.06$	2	$.06$	1	$.19$	809 ± 2	$5/2^-$
							825.6	$1/2^-(3/2^-)$
							895 ± 2	$1/2^-(3/2^-)$
							912.1	$1/2^-(3/2^-)$

Table 5 - Continued.

E_x (keV)	$^{74}\text{Ge}(p,d)$ Present Work		$^{74}\text{Ge}(p,d)$ Fournier et al. 18)		$^{72}\text{Ge}(d,p)$ Kato, 16) Hasselgren ³⁾ Heyman et al. 15)		Combined Results for ^{73}Ge ^{b)}	
	λ	C^2S	λ	C^2S	λ	C^2S	E_x (keV)	J^π
(934)							929.5	$(1/2, 3/2)$
							951.9	
(1026) ^{a)}							(1026±5)	
1044	1	.44	1	.45	1	.24	1041.7	$3/2^-(1/2^-)$
1133	1	.02	3	.64	1	.23	1131.9	$1/2^- + 5/2^-$
	3	.14						
1153 ^{a)}	3	.62					1153±3	$5/2^-$
1192	3	.29	3	.62			1192±3	$5/2^- + 9/2^+$
	4	.25						
1265	1	.08	1	.12			1259.6	$3/2^-(1/2^-)$
							1274±10	$1/2^-$
1311	1	.13	1	.17	0		1311±5	$3/2^-(1/2^-)$
							1329±10	
							1376±10	
1528 ^{a)}	3	.14					1528±4	$5/2^-$
							1597±10	$1/2^+$
1611	3	.39	3	.78	(0)	.1	1611±7	$5/2^- + 9/2^+$
	4	.21						
1635	2	.05	1	.07	2	1.13	1635±5	$5/2^+$
							1646±10	$5/2^+$
1744	0	.01	2	.06	0	.67	1744±5	$1/2^+$
1756					4	.86	1756±5	$9/2^+$

Table 5 - Continued.

E _x (keV)	74Ge(p,d) Present Work		74Ge(p,d) Fournier et al. 18)		72Ge(d,p) Kato, 16) Hasselgren 3) Heyman et al. 15)		Combined Results for 73Ge b)	
	ℓ	C ² S	ℓ	C ² S	ℓ	C ² S	E _x (keV)	J ^π
2036	1	.14	1	.18	(2)	.11	2036±5	3/2(1/2) ⁻
2101	(2)	.01			0	.24	2101±5	3/2(1/2) ⁻
2131 ^a	1	.05			2	.27	2131±5	5/2 ⁺
2145 ^a	2	.02					2145±5	3/2(1/2) ⁻
2185 ^a	1	.01			2	.24	2185±5	5/2 ⁺
2267			1	.05	2	.12	2225±10	3/2(1/2) ⁻
2335	1	.06	1	.1	2	.08	2267±7	3/2(1/2) ⁻
					0		2320±10	3/2(1/2) ⁻
							2335±5	3/2(1/2) ⁻
							2374±10	3/2(1/2) ⁻
							1804±10	5/2 ⁺
							1911±10	(5/2 ⁺)
							1936±10	3/2 ⁻
							1960±10	(5/2 ⁺)
							1983±10	3/2 ⁻
							1995±10	(5/2 ⁺)
							2010±10	(5/2 ⁺)
							2024±10	(5/2 ⁺)
							2066±10	3/2(1/2) ⁻
							2101±5	1/2 ⁺
							2131±5	5/2 ⁺
							2145±5	3/2(1/2) ⁻
							2185±5	5/2 ⁺
							2225±10	3/2(1/2) ⁻
							2267±7	(5/2 ⁺)
							2320±10	3/2(1/2) ⁻
							2335±5	(5/2 ⁺)
							2374±10	3/2(1/2) ⁻

Table 5 - Continued.

E_x (keV)	$^{74}\text{Ge}(p,d)$ Present Work		$^{74}\text{Ge}(p,d)$ Fournier et al. 18)		$^{72}\text{Ge}(d,p)$ Kato, 16) Hasselgren ³⁾ Heyman et al. 15)		Combined Results for ^{73}Ge ^{b)}	
	λ	C^2S	λ	C^2S	λ	C^2S	E_x (keV)	J^π
2462					1		2411 \pm 10	3/2(1/2) $^-$
2482	1	.04			0	.32	2462 \pm 7	1/2 $^+$
2508 ^{a)}	1	.04				weak	2482 \pm 7	3/2(1/2) $^-$
2564 ^{a)}	1	.03					2508 \pm 7	3/2(1/2) $^-$
					2	.3	2564 \pm 7	3/2(1/2) $^-$
2678 ^{a)}	1	.01			(2)	.1	2580 \pm 10	(5/2 $^+$)
					(2)	.08	2618 \pm 10	(5/2 $^+$)
2696 ^{a)}	1	.02			(2)	.08	2678 \pm 7	3/2(1/2) $^-$
							2683 \pm 10	(5/2 $^+$)
2743	2	.01			0	.08	2696 \pm 7	3/2(1/2) $^-$
2796 ^{a)}	3	.14			2	.34	2732 \pm 10	1/2 $^+$
2831 ^{a)}							2743 \pm 7	5/2 $^+$
							2796 \pm 7	5/2 $^-$
					(2)	.11	2831 \pm 7	
						weak	2846 \pm 10	(5/2 $^+$)
					0	.3	2860 \pm 10	
					0	.03	2915 \pm 10	1/2 $^+$
					0		2931 \pm 10	1/2 $^+$

Table 5 - Continued.

E_x (keV)	$^{74}\text{Ge}(p,d)$ Present Work		$^{74}\text{Ge}(p,d)$ Fournier et al. 18)		$^{72}\text{Ge}(d,p)$ Kato, 16) Hasselgren 3) Heyman et al. 15)		Combined Results for ^{73}Ge b)	
	λ	C^2S	λ	C^2S	λ	C^2S	E_x (keV)	J^π
3017 ^{a)}	1	.01					3017 \pm 7	3/2(1/2) ⁻
3037	1	.02			weak		3037 \pm 7	3/2(1/2) ⁻
3058 ^{a)}	1	.01			weak		3058 \pm 7	3/2(1/2) ⁻
3172	1	.02			weak		3172 \pm 7	3/2(1/2) ⁻
					weak		3223 \pm 10	
					weak		3277	
3356	1	.02			weak		3356 \pm 7	3/2(1/2) ⁻
3384 ^{a)}							3384 \pm 7	
			2	.11		(5/2 ⁺)	3418 \pm 10	(5/2 ⁺)
			(0)	.03		(1/2 ⁺)	3514 \pm 10	(1/2 ⁺)
			(0)	.07		(1/2 ⁺)	3551 \pm 10	(1/2 ⁺)
3623 ^{a)}	1	.01					3623 \pm 10	3/2(1/2) ⁻ +5/2 ⁻
	3	.03						
3631 ^{a)}							3631 \pm 7	
3703 \pm 7 ^{a)}							3703 \pm 7	
			(2)	.04		(5/2 ⁺)	3727 \pm 10	(5/2 ⁺)
			(2)	.02		(5/2 ⁺)	3766 \pm 10	(5/2 ⁺)
					weak		3805 \pm 10	
3805*					weak		3849 \pm 10	

Table 5 - Continued.

E _x (keV)	7 ⁴ Ge(p,d) Present Work		7 ⁴ Ge(p,d) Fournier et al. 18)		7 ² Ge(d,p) Kato, 16) Hasselgren ³⁾ Heyman et al. 15)		Combined Results for 7 ³ Ge ^{b)}	
	λ	C ² S	λ	C ² S	λ	C ² S	E _x (keV)	J ^π
3924	1	.01					3924±7	3/2(1/2) ⁻
3945 ^{a)}							3945±7	
4000 ^{a)}							4000±7	
4059 ^{a)}							4059±7	
4073 ^{a)}							4073±7	
4370 ^{a)}							4370±7	
4437 ^{a)}							4437±7	
4569 ^{a)}							4569±7	
4601 ^{a)}							4601±7	
4653 ^{a)}							4653±7	
4667 ^{a)}							4667±7	
						weak		

* Doublet.

a) States seen for the first time in the present work.

b) Compiled from the results of the present work, and those of references 3, 15, 16, and 26.

c) Uncertainties are ±1 keV for energies quoted to tenth keV accuracy.

Figure 13. Experimental angular distributions obtained for the $^{74}\text{Ge}(p,d)$ reaction at 35 MeV. The solid lines are fits to the data of DWBA predictions. For mixed ℓ -transfers, the dashed lines show the contribution of each component.

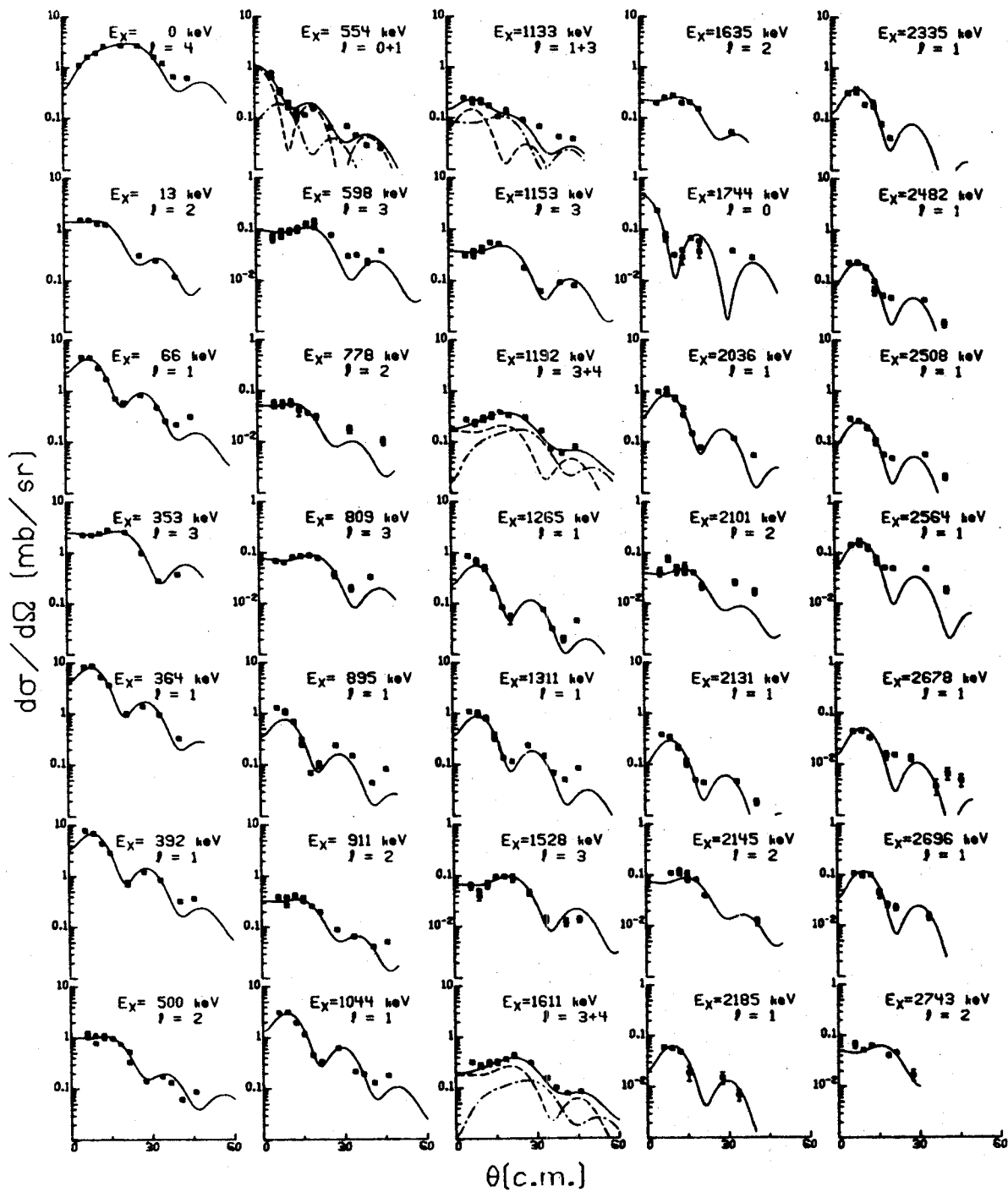


Figure 13

Figure 14. Experimental angular distributions obtained from the $^{74}\text{Ge}(p,d)$ reaction at 35 MeV. The solid curves are fits to the data of DWBA predictions. For mixed ℓ -transfers, the dashed lines show the contribution of each component.

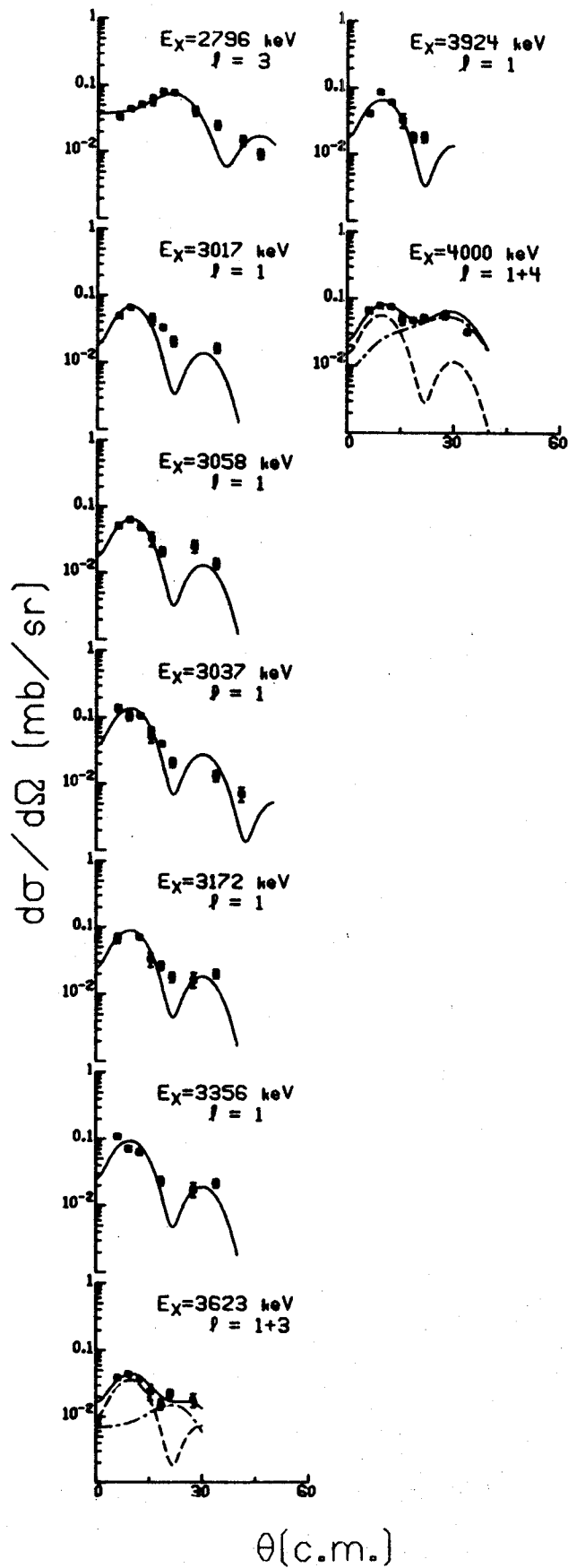


Figure 14

to (d,p) strength is ambiguous and the γ -ray work gives no information, but two other considerations favor the $3/2$ assignment. First, a $J=1/2$ assignment leaves us with too much $2p_{1/2}$ strength relative to the other isotopes, and second, $J=3/2$ fits in with the $\ell=1$ systematics as previously mentioned.

500 keV state: We observe a pure $\ell=2$ transition to this state which is in agreement with the results of the (d,p) reaction. Fournier et al.¹⁸⁾ fit the angular distribution for this state with an $\ell=1+2$ mixture which implies that there are two close states here. We see no evidence for an $\ell=1$ component to the transition and our spectra show no evidence for a second state near this energy. Actually, the angular distribution for this state that is shown in Reference 18 is almost indistinguishable from the pure $\ell=2$ shape which is shown fitted to the 557 keV angular distribution. It is, therefore, doubtful that there is an $\ell=1$ component to this transition.

554 keV state: In our spectra the peak for the $^{72}\text{Ge}(p,d)$ $\ell=1$ transition to the ground state of ^{71}Ge falls right on top of the peak for this state. In the figure we show a fit to the sum of these transitions using an $\ell=0+1$ mixture which allows us to extract the spectroscopic factor for this state. The resulting fit is good, supporting an $\ell=0$ assignment for the transition to this state in agreement with the (d,p) results. Fournier et al.,¹⁸⁾ however, report an $\ell=2$ transfer for this transition. It is possible that in the previous (p,d)

work the impurity was not subtracted out correctly. Also, the forward angle rise may have been missed since no data was taken at angles less than 15° . These two factors could then cause an error in determining the ℓ -transfer.

912 keV state: Our data show a fairly weak but distinct $\ell=2$ transition to this state. This is in disagreement with the (d,p) $\ell=1$ transition to this state reported by Hasselgren.³⁾ The energy calibrations indicate that the two reactions are populating states at the same energy, although it may be possible that the (d,p) reaction is populating the 929 keV state. According to the γ -ray spin assignment, the 929 keV state should be populated by an $\ell=1$ transfer. Another possible explanation is that this state is a doublet and each reaction is populating only one member.

1133 keV state: This state also appears to be a doublet despite the lack of evidence for two states at this energy in the spectra. Our angular distribution is only fit well with an $\ell=1+3$ mixture, with the $\ell=3$ component dominating the transition. Fournier et al.¹⁸⁾ show an $\ell=3$ fit to the transition but the experimental shape is not well reproduced. Also, the 15° point shows indications of a possible rise at forward angles. Hasselgren³⁾ quotes a pure $\ell=1$ (d,p) shape for this transition. Thus, the angular distributions of both (p,d) experiments combined with the (d,p) experiment give evidence for this state being a doublet. However, the state is weakly populated and it is possible that there is no $\ell=1$ component

to the (p,d) transition. Hasselgren³⁾ does not show an angular distribution for this state so we cannot comment on its quality

1192 keV and 1611 keV doublets: Although there is no evidence from the spectra for either of these states being a doublet, we deduce that they are based on the fact that the angular distributions can only be fitted by an $\ell=3+4$ mixture. Indeed the shapes of the angular distributions are very similar to that of the transition to the 1699 keV state in ⁷⁵Ge which is observed to be a doublet from the spectra and is fit by an $\ell=3+4$ mixture. Fournier et al.¹⁸⁾ also have trouble fitting these distributions with $\ell=3$ shapes, although their other $\ell=3$ and $\ell=4$ transitions are fitted well. It appears that these distributions shown in Reference 18 would only be fit well by an $\ell=3+4$ mixture. Pure $\ell=4$ assignments to these transitions yield a summed $\ell=3$ spectroscopic factor that is too small relative to the results of the (p,d) reaction on the other isotopes, while either an $\ell=3+4$ mixture or a pure $\ell=3$ transition gives consistent results. A pure $\ell=3$ transition is doubtful since both (p,d) experiments show the distortion.

Aside from assuming that these states are doublets one might try to explain the shapes in other ways. One possibility is that these are really $7/2^-$ states and the distortion is due to the J-dependence in the shape of the angular distributions. Sherr et al.²⁸⁾ have observed an $\ell=3$ J-dependence in the ⁵⁶Fe(p,d) reaction at 28 MeV and more recently Nolan²⁹⁾

and Kong³⁰⁾ have seen it on the (p,d) reaction on the nickel isotopes at 35 MeV. This J-dependence is characterized by three effects:

1. DWBA calculations fit the $7/2^-$ transitions but not the $5/2^-$ transitions.
2. The $5/2^-$ transitions have the first maximum shifted by about 3° toward lower angles relative to the $7/2^-$ transitions.
3. The $7/2^-$ transitions exhibit a less pronounced diffraction pattern (i.e., the minima are filled in).

The shapes we observe for these states would be consistent with 2) and 3) but not with 1). Our $\ell=3$ DWBA calculations fit the distributions for transitions to known $5/2^-$ states very well, but do not fit these shapes. It is possible of course that the J-dependence effect is dependent on the relative filling of the $1f_{5/2}$ and $1f_{7/2}$ orbits in which case we would not expect that the effect seen in the nickel region would be reproduced exactly in the germanium region. However, our summed $\ell=3$ spectroscopic factors (assuming these transitions to be pure $\ell=3$, $j=5/2$) do not indicate more strength than we would expect to see from the sum rule limit for the $1f_{5/2}$ orbit, and finally, we would not expect to see significant $1f_{7/2}$ strength at this low an excitation energy. Another possibility is that these shapes are the result of a multi-step process. We cannot rule out this possibility but it

would seem that we should see more evidence of it if multi-step processes were important enough to produce the effect seen in these distributions as these transitions are fairly strong.

1744 keV state: The transition to this state is quite weak, as would be expected for an $\ell=0$ transfer, but the shape is definitely that of an $\ell=0$ transition. This is in agreement with the (d,p) work. Fournier et al.¹⁸⁾ report an $\ell=2$ transfer to this state, but would not have resolved it from the weak peak of the 1756 keV state. This, coupled with the poor statistics and lack of data points below 15° , probably accounts for the discrepancy.

2101 keV state: Kato¹⁶⁾ reports a possible $\ell=0$ transfer for this state but shows no angular distribution for the transition. Our data is not very complete for this state, as the transition is quite weak, but there is no evidence for an $\ell=0$ component and the $\ell=2$ transfer we observe is in agreement with Hasselgren's (d,p) results.³⁾ It is, therefore, likely that the $\ell=2$ assignment is correct.

Fournier et al.¹⁸⁾ report states at 730 keV and 1653 keV, but in both cases our data indicates that these peaks would be covered by a peak resulting from the (p,d) reaction on one or the other germanium isotopes. For the one case (1653 keV state) where an ℓ -value is reported for the transition, it is the same as that which would populate the impurity. As previously mentioned, the purity of the targets used in

the previous (p,d) work is comparable to ours. Therefore, it is doubtful that there are states in ^{73}Ge at these energies.

VIII. THE $^{76}\text{Ge}(p,d)^{75}\text{Ge}$ REACTION

VIII.1 General Comments

The results for this reaction are summarized in Table 6 and the angular distributions are shown in Figure 15. The second plate showed no peaks stronger than 15 $\mu\text{b}/\text{sr}$ at 6° between 4 MeV and 9 MeV excitation. In general, excitation energies, ℓ -values, and spectroscopic factors obtained in the present study are in good agreement with those of previous work. It is, however, difficult to make comparisons with the (d,p) work except at low excitation energies because at higher excitation energies the (d,p) reaction mostly populates states by $\ell=2$ and $\ell=0$ transfers.

In doing the excitation energy analysis it was necessary to adjust the Q-value for this reaction by +11 keV. This indicates a +11 keV correction to the quoted²¹⁾ mass of ^{75}Ge since we expect the mass of ^{76}Ge (a stable nucleus) to be accurately known. This new mass is consistent (within 2 keV) with the mass for ^{75}Ge determined from the $^{74}\text{Ge}(n,\gamma)$ Q-value measured by Hasselgren.³⁾

There again appears to be a slight variation in the $1/2^-$, $3/2^-$ systematics in this nucleus. There is a fairly weak ($S=.17$) state which is assumed to have a spin of $1/2^-$. The $1/2^-$ assignment is preferred by Kato¹⁶⁾ in the (d,p) reaction and by the ratio of strengths argument. If the state does indeed have a spin of $1/2^-$, it has no counterpart in the other

Table 6. Summary of results for states in ^{75}Ge .

$E_x(\text{keV})$	$^{76}\text{Ge}(\text{p,d})$ Present Work		$^{76}\text{Ge}(\text{p,d})$ Fournier, et al. 18)		$^{74}\text{Ge}(\text{d,p})$ Kato ¹⁶ & Hasselgren ³⁾		Combined Results for $^{75}\text{Ge}(\text{b})$	
	λ	C^2S	λ	C^2S	λ	C^2S	$E_x(\text{keV})^c$	J^π
0	1	.65	1	.61	1	.62	0	$1/2^-$
139	4	.16				weak	62 ± 5	$7/2^+$
197*	4	4.75	2	.42	4	4.3	180 ± 5	$9/2^+$
			4	4.2			197 ± 5	
253	1	.17	1	.16	1	.15	253.1	$1/2^-$
317	3	2.17	3	1.38	3	1.21	317 ± 2	$5/2^-$
							326 ± 5	
							360 ± 5	
457	3	.33	3	.32	0		453 ± 5	$1/2^+$
576	1	1.58	1	1.59	1	weak	457 ± 2	$5/2^-$
585	2	.25	3	1.59	2	1.31	575.6	$3/2(1/2)^-$
651 ^{a)}	3	.05					584.2	$5/2^+$
675	0	.01	2	.05	0	.043	651 ± 2	$5/2^-$
886	1	.16	1	.14	1	.25	675 ± 2	$1/2^+$
							884.8	$1/2(3/2)^-$
							940 ± 10	
988				weak		weak	988 ± 3	
					0	.02	1226 ± 10	$1/2^+$
					2	.34	1136.8	$(5/2^+)$
1242	3	.25		weak		weak	1242 ± 3	$5/2^-$

Table 6 - Continued.

E _x (keV)	76Ge(p,d) Present Work		76Ge(p,d) Fournier, et al. 18)		74Ge(d,p) Kato 16) & Hasselgren 3)		Combined Results for 75Ge b)	
	ℓ	J ^π	ℓ	C ² S	ℓ	C ² S	E _x (keV) c)	J ^π
1258	(4)	.32		(9/2 ⁺)			1258±3	(9/2 ⁺)
1396	2	.08		5/2 ⁺			1320±10	
1417	1	.19	1	3/2(1/2) ⁻	2	.32	1396±3	5/2 ⁺
			3	3/2(1/2) ⁻			1417±5	3/2(1/2) ⁻
1503	1	.50	1	3/2(1/2) ⁻			1470±10	
1539 ^a	2	.05		5/2 ⁺	0	.55	1503±5	3/2 ⁻ (1/2) ⁻
1603	3	.76		5/2 ⁻	4	.27	1509±5	1/2 ⁺
1699*	3	.21	3	5/2 ⁻			1534±5	(9/2 ⁺)
	4	.19	3	9/2 ⁻			1539±5	5/2 ⁺
				5/2 ⁻			1603±5	5/2 ⁻
1800	1	.22	1	3/2(1/2) ⁻	2	.94	1699*±5	5/2 ⁻ +9/2 ⁻
1869							1712±10	(5/2 ⁺)
							1740±10	
							1800±5	3/2(1/2) ⁻
							1854±7	(5/2 ⁺)
							1869±5	(5/2 ⁺)
							2002	(5/2 ⁺)
							2050±10	
							2105±10	(1/2 ⁺)
							2136±10	
							2193±5	1/2 ⁺

Table 6 - Continued.

E _x (keV)	76Ge(p,d) Present Work		76Ge(p,d) Fournier, et al. 18)		74Ge(d,p) Kato 16) & Hasselgren 3)		Combined Results for 75Ge b)	
	ℓ	C ² S	ℓ	C ² S	ℓ	C ² S	E _x (keV) c)	J ^π
2281 a)							2212±5	
							2230±10	
							2281±5	
2323	1	.19	3/2(1/2) ⁻	1	.18	3/2(1/2)	2310±7	1/2 ⁺
2359	1	.04	3/2(1/2) ⁻				2323±5	3/2(1/2) ⁻
2382	4	.4	9/2 ⁺				2359±5	3/2(1/2) ⁻
							2382±5	9/2 ⁺
							2410±10	(5/2 ⁺)
							2462±10	
2534	3	.22	5/2 ⁻				2527±10	(5/2 ⁺)
2572	1	.03	3/2(1/2) ⁻				2534±5	5/2 ⁻
							2572±5	3/2(1/2) ⁻
2681*	1	.12	3/2(1/2) ⁻	1	.11	3/2(1/2) ⁻	2637±10	1/2 ⁺
							2660±10	1/2 ⁺
2829 a)							2681*±7	3/2(1/2) ⁻
2857* a)							2725±10	1/2 ⁺
2954 a)							2829±7	
3067 a)							2857*±7	
3165 a)							2954±7	
							3067±7	
							3165±7	

Table 6 - Continued.

E_x (keV)	$^{76}\text{Ge}(p,d)$ Present Work		$^{76}\text{Ge}(p,d)$ Fournier, <u>et al.</u> 18)		$^{74}\text{Ge}(d,p)$ Kato 16) & Hasselgren 3)		Combined Results for ^{75}Ge			
	λ	C^2S	J^π	λ	C^2S	J^π	λ	C^2S	E_x (keV) c)	J^π
3182 ^{a)}	1	.036	$3/2(1/2)^-$						3182 \pm 7	$3/2(1/2)^-$
3194 ^{a)}									3194 \pm 7	$3/2(1/2)^-$
3272 ^{a)}									3272 \pm 7	
3385 ^{a)}									3385 \pm 7	
3451 ^{a)}									3451 \pm 7	
3494 ^{*a)}									3494 \pm 7	
3626 ^{*a)}	1	.03	$3/2(1/2)^-$						3626 \pm 7	$3/2(1/2)^-$
3719 ^{a)}									3	.03
3839 ^{a)}									3839 \pm 7	

* Doublet.

a) States seen for the first time in the present work.

b) Compiled from the results of the present work and those of references 3, 16, and 26.

c) Uncertainties are ± 1 keV for those energies quoted to a tenth of a keV.

Figure 15. Experimental angular distributions obtained from the $^{76}\text{Ge}(p,d)$ reaction at 35 MeV. The solid curves are fits to the data of DWBA predictions. For mixed ℓ -transfers, the dashed lines show the contribution of each component.

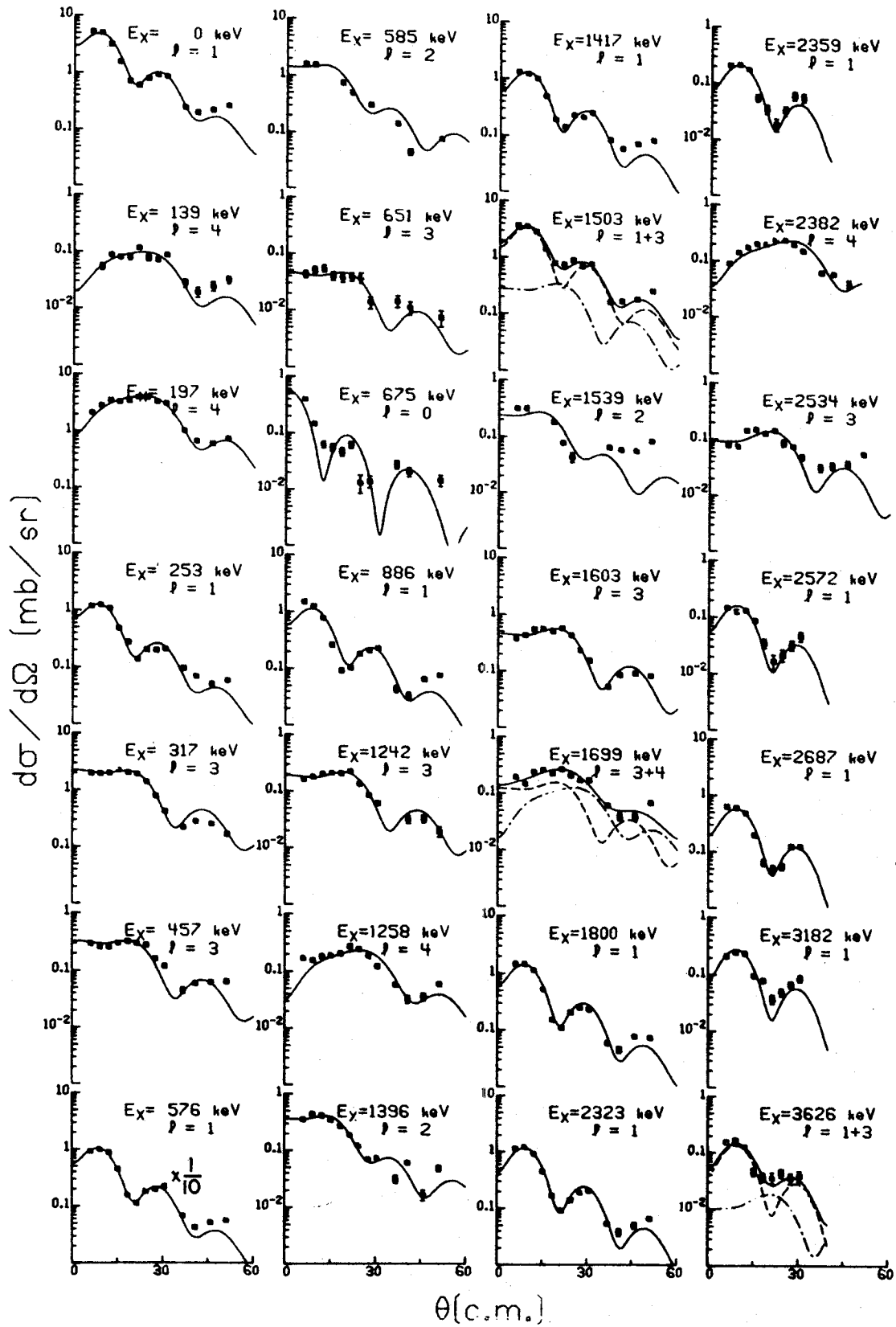


Figure 15

om
urves

odd nuclei. However, the spin is not firmly established and it could well be that the spin is actually $3/2^-$. This would then be more consistent with the systematics as ^{69}Ge has a weak $3/2^-$ state at 233 keV.

VIII.2 Comments on Individual States

139 keV state: We observe an $\ell=4$ transition to this state which would initially suggest a $9/2^+$ spin assignment. However, life-time and conversion coefficient measurements suggest a spin assignment of $7/2^+$.³¹⁾ There are other "anomalous" $7/2^+$ states in neighboring nuclei²⁶⁾ which have been attributed to $(1g_{9/2})^3$ configurations.²⁶⁾ In particular there is the 68.2 keV state in ^{73}Ge with a probable spin of $7/2^+$. The fact that we observe the 139 keV state in our data indicates that there is some population of the $1g_{7/2}$ orbit on ^{76}Ge . It also indicates that the wave function of the 139 keV state includes a component with a $(1g_{7/2})^1$ term. The state is nevertheless quite likely dominated by the $(1g_{9/2})^3$ configuration since it is not observed in the (d,p) reaction. Since we do not observe the 68.2 keV state in ^{73}Ge (it would be covered by the strong transition to the 66.7 keV state) we cannot make comparisons as to the relative $1g_{7/2}$ population in ^{74}Ge and ^{76}Ge . Neither can we deduce anything about the wave function of the 68.2 keV state in ^{73}Ge .

197 keV doublet: This peak is clearly observed to be a doublet in the spectra at 6° , 9° , and 12° by a (one or two channel) broadening in the peak. This is reflected in the

angular distribution by a rise above the pure $\ell=4$ shape at these angles. This same deviation occurs in the angular distribution shown by Hasselgren³⁾ and to a lesser degree those of Fournier et al.¹⁸⁾ and Kato.¹⁶⁾ In our data the deviation is so slight that the fit is not significantly improved by adding in another ℓ -component. For this reason, we cannot distinguish between an $\ell=1+4$ or an $\ell=1+3$ mixture for this transition, although the $\ell=1+4$ fit is slightly better. The energy separation between the states of this doublet is about 7 keV. The lower member may be the same state as the 180 keV state reported in the Nuclear Data Sheets, but if it is, the 180 keV energy is too low.

457 keV state: Our data show a distinct $\ell=3$ transition to this state which is in agreement with the (p,d) results of Fournier et al.¹⁸⁾ Hasselgren³⁾ observes a state in the (d,p) reaction at 457 keV, but gives no ℓ -transfer for the transition. However, Kato¹⁶⁾ reports a state at 453 keV which is listed in the table as being populated by an $\ell=2$ transfer and is shown in the figure with an $\ell=0$ angular distribution. Either an $\ell=0$ or an $\ell=2$ assignment would be in disagreement with our data. At this low an excitation energy the energy calibrations for the different experiments are sufficiently consistent that either this state must be a close doublet or there has been an error in assigning ℓ -transfers. The agreement in the two (p,d) experiments supports the $\ell=3$ assignment for this reaction. However, the confusion between figure

and table in Reference 16 and the lack of any ℓ -transfer assignment in Reference 3 makes it impossible to give a meaningful critique of the (d,p) ℓ -transfer assignment.

585 keV state: We observe an $\ell=2$ transfer to this state which is in agreement with the (d,p) results of Kato.¹⁶⁾ Fournier et al.¹⁸⁾ did not resolve this state from the 576 keV state and fit the sum of the angular distributions with an $\ell=1+3$ mixture. However, the summed distribution is dominated by the $\ell=1$ component and it appears that it could be fit acceptably by an $\ell=1+2$ mixture. This would then be in agreement with the (d,p) results and with our (p,d) data.

675 keV state: We observe a distinct $\ell=0$ transition to this state which is in agreement with the (d,p) results of Hasselgren.³⁾ Kato¹⁶⁾ again shows a discrepancy between figure and table, but the figure shows an $\ell=0$ transition. In disagreement with these results is the $\ell=2$ transition reported by Fournier et al.¹⁸⁾ This contradiction is probably due to the fact that the previous (p,d) work did not resolve the 651 keV state from this state and therefore obtained an angular distribution which is actually an $\ell=0+3$ mixture.

1258 keV state: The uncertainty in the ℓ -transfer assignment for this state is due to the fact that angular distribution is not fit as well as the other $\ell=4$ transitions we see. A small $\ell=3$ component would improve the fit, but not significantly enough to warrant calling this state a doublet.

1417 keV state: There is slight evidence in our spectra that this state is actually a doublet. However, the angular distribution is fit very well by a pure $\ell=1$ shape which indicates that if there are two states here, they are both populated by $\ell=1$ transfers. Fournier et al.¹⁸⁾ fits the angular distribution for this state with an $\ell=1+3$ mixture, but did not resolve the 1396 keV state which is populated by an $\ell=2$ transition. This resolves the contradiction since the angular distribution shown in Reference 18 is dominated by the $\ell=1$ component and it appears that it would be fit acceptably by an $\ell=1+2$ mixture.

1699 keV doublet: There is a consistent one channel broadening of the peak for this state in our spectra which indicates a doublet of about 5 or 6 keV separation. The angular distribution also indicates a doublet as it can only be fitted well by an $\ell=3+4$ mixture. Fournier et al.¹⁸⁾ fit the angular distribution for this state with a pure $\ell=3$ shape, but the fit is not good. It appears that the angular distribution shown in Reference 18 is consistent with our data in that it would be fit well by an $\ell=3+4$ mixture.

2359 keV and 2382 keV states: Both of these states are weakly populated in the (p,d) reaction, but the angular distributions are distinct and are well fitted by an $\ell=1$ and an $\ell=4$ shape respectively. The (d,p) work appears to be in contradiction to our results as Kato¹⁶⁾ reports an $\ell=2$ transition to a state at 2359 keV and Hasselgren³⁾ reports an $\ell=2$ transition

to a state at 2382 keV. However, neither Hasselgren nor Kato report seeing both states. Also, there is a growing discrepancy starting at about 1800 keV as to the energy of the states seen, and even which states are populated, in the (d,p) reaction. It is likely that the energy calibrations in the two (d,p) experiments are not consistent, and that the states reported by Hasselgren³⁾ at 2321 keV, 2382 keV, 2527 keV, 2574 keV, and 2660 keV are the same as those reported by Kato¹⁶⁾ at 2310 keV, 2359 keV, 2462 keV, 2553 keV, and 2636 keV. Equating these states would present no contradictions in ℓ -transfers between the two (d,p) experiments. This would help to explain the contradiction between the (p,d) and (d,p) results for the 2359 keV and 2382 keV states. It is possible that these states were not resolved in the (d,p) work and the $\ell=1+4$ was mistaken for an $\ell=2$ transition. If the $\ell=2$ assignment is indeed correct, then the (d,p) reaction must be populating a different state from the ones we observe in the (p,d) reaction.

2323 keV and 2572 keV states: Our data show definite $\ell=1$ transitions to both of these states. Hasselgren³⁾ reports $\ell=2$ transitions to states at 2321 keV and 2574 keV which would be in disagreement with our results. However, as has already been pointed out, the energy calibration in the (d,p) work is suspect and it is therefore not at all obvious that the same states are being seen in both the (p,d) and (d,p) reaction. If these two states are the same in both reactions, then the $\ell=2$ assignment is probably incorrect,

since the angular distributions shown in Reference 3 would be fitted well by the empirical $\ell=1$ shape of the 252 keV state. Fournier et al.¹⁸⁾ report states at 2043 keV, 2105 keV, and 2198 keV. However, these states would all be covered by peaks from germanium isotopes that are populated by the same ℓ -transfers, and with approximately the same strength as reported for these states. It is, therefore, doubtful that there are states in ^{75}Ge at these energies.

IX. DISCUSSION OF RESULTS

IX.1 General Features

Figures 16-21 show the general features of the results of the present study. Figure 16, which was referred to in Chapter IV, shows the distribution of the strong transitions to states in the odd isotopes. Figures 17-21 show energy level diagrams for each of the nuclei studied. Here we show the previously observed states up through 2 MeV excitation and the states we observe in the (p,d) experiment. We observe most of the states previously reported up to this excitation energy.

IX.2 Summed Spectroscopic Factors

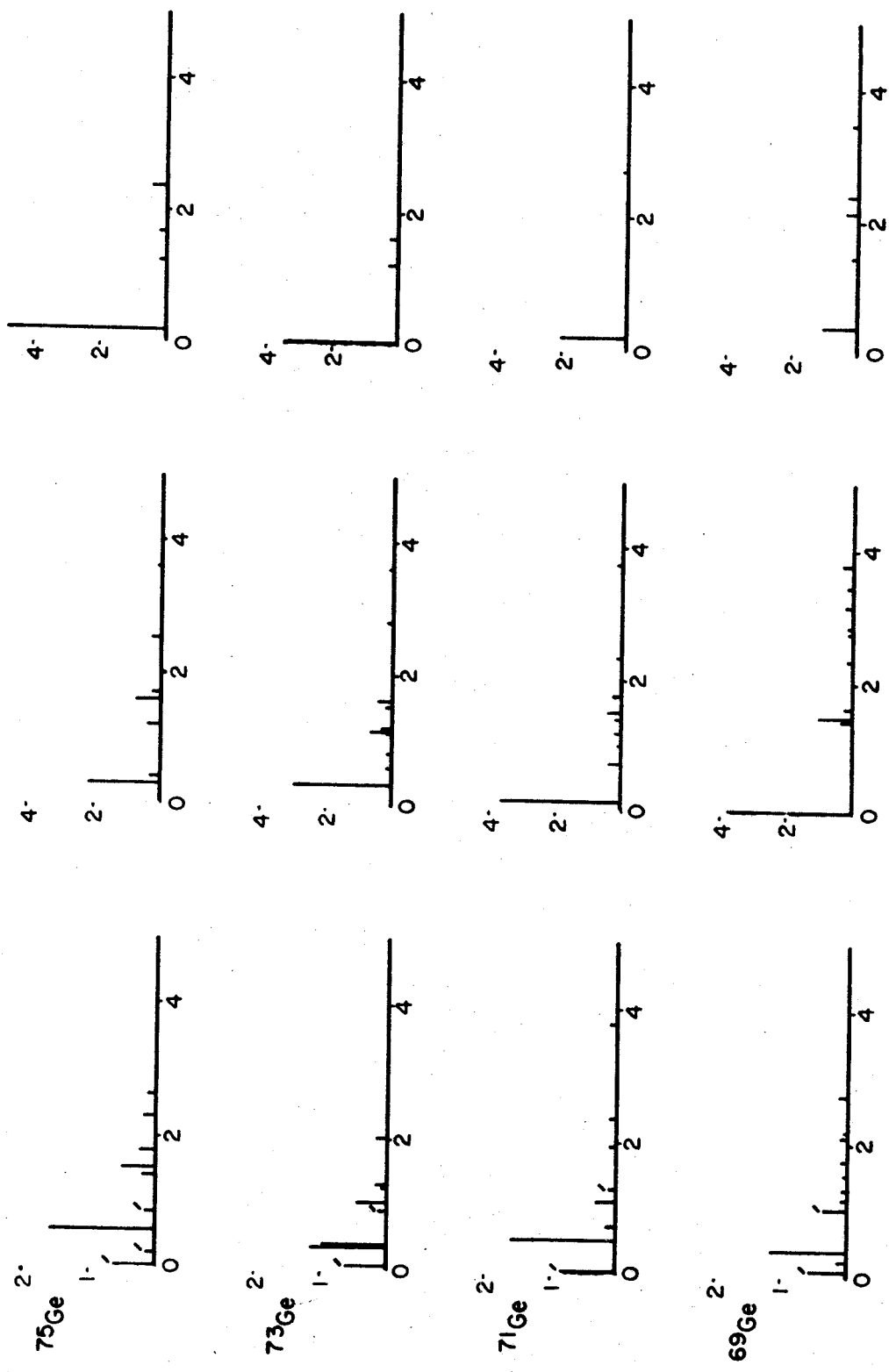
It was mentioned in the Introduction that the sum of the spectroscopic factors for a given l - j transfer is a measure of the number of particles in that orbit. The maximum number of neutrons allowed in an orbit is given by $2j + 1$ where j is the total angular momentum of the neutrons in that orbit. (The same relation holds for protons.) This then gives a sum-rule limit for the spectroscopic factors for pickup from that orbit. The situation is complicated a little bit however by isotopic spin considerations. Isotopic spin (T) is primarily a measure of the relative number of protons and neutrons in a nucleus and it obeys quantum mechanical angular momentum algebra. Indeed for all states of all

Figure 16. Spectroscopic strength plotted as a function of excitation energy for ℓ -transfers of 1, 3, and 4 for the (p,d) reaction on the even targets.

$l = 4$

$l = 3$

$l = 1$



EXCITATION ENERGY (MeV)

Figure 16

Figure 17. Energy level diagram for states below 2 MeV in ^{69}Ge showing energy, ℓ -transfer, spectroscopic factor, and sample spectrum for states populated in the (p,d) reaction.

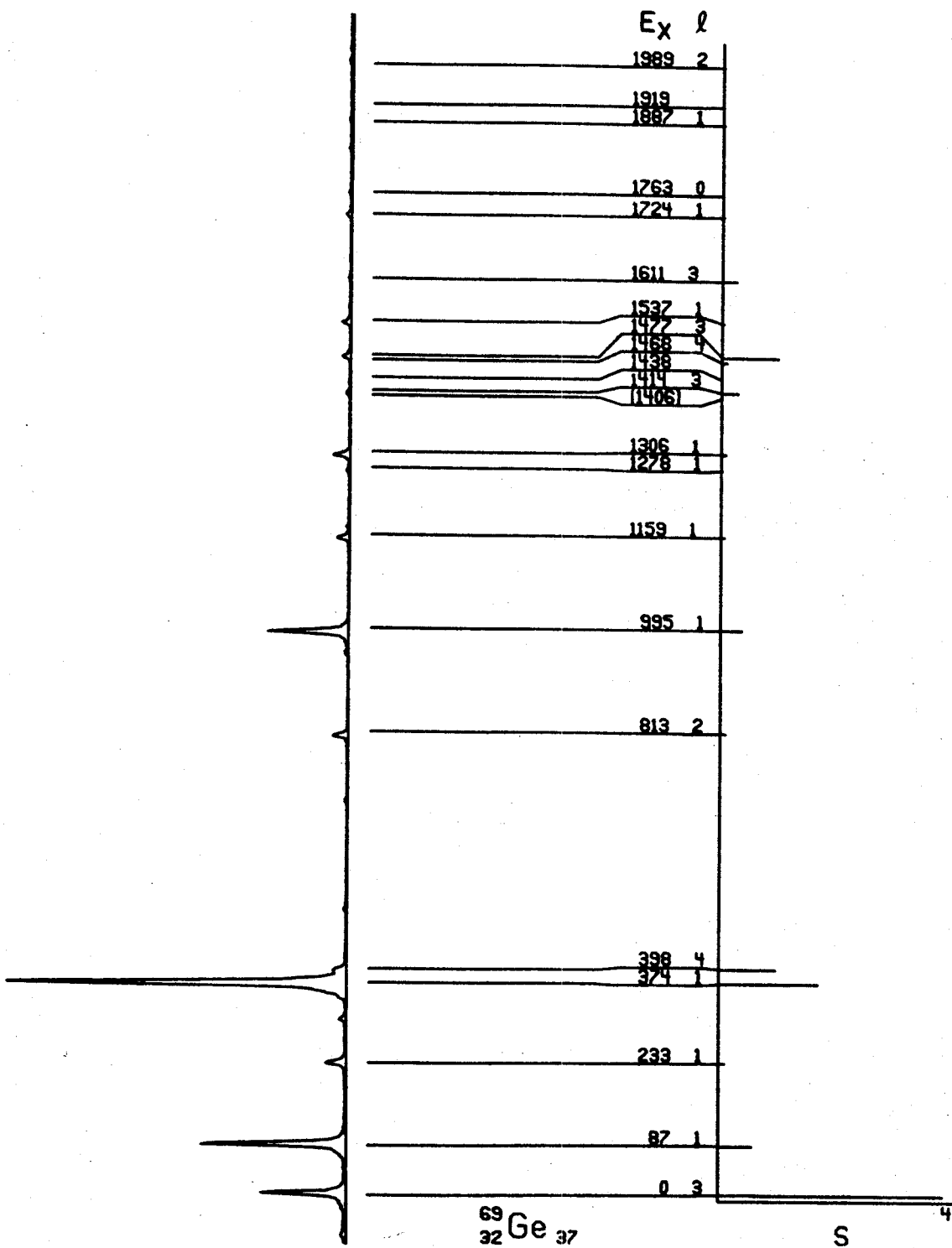


Figure 17

Figure 18. Energy level diagram for states below 2 MeV in ^{71}Ge showing energy, l -transfer, spectroscopic factor, and sample spectrum for states populated in the (p,d) reaction.

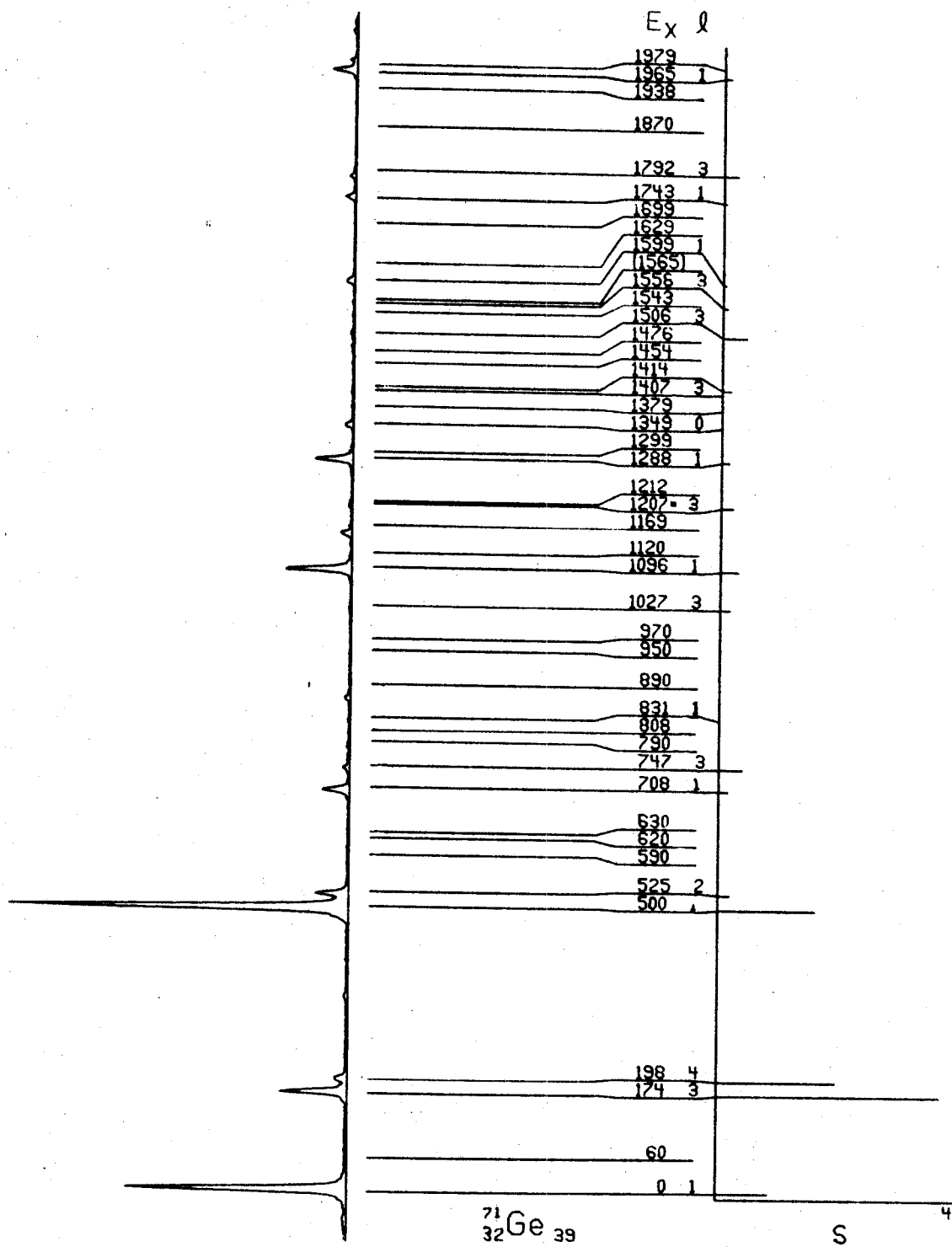


Figure 18

Figure 19. Energy level diagram for states below 3.5 MeV in ^{72}Ge showing energy, l -transfer, spectroscopic factor, and sample spectrum for states populated in the (p,d) reaction.

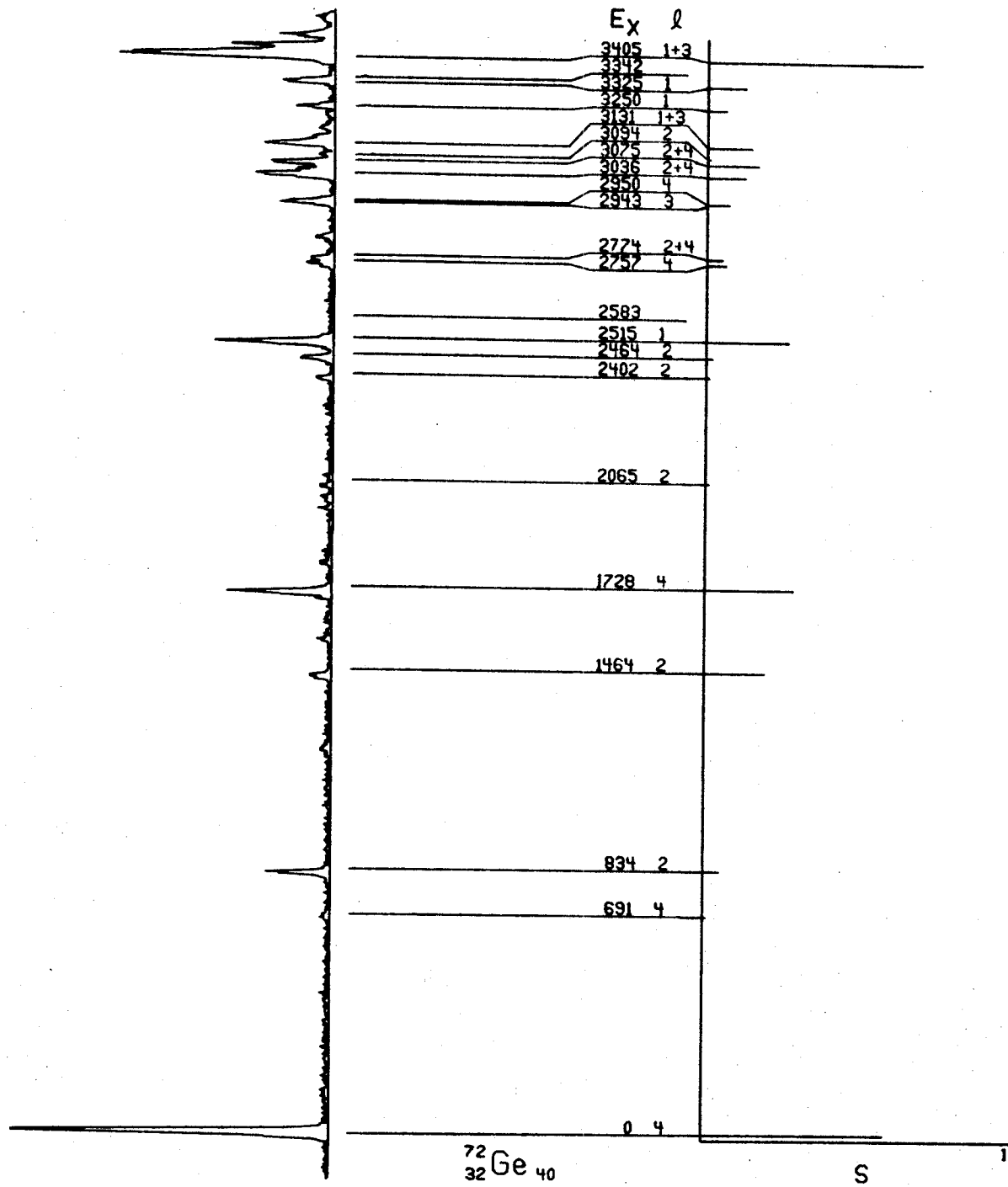


Figure 19

Figure 20. Energy level diagram for states below 2 MeV in ^{73}Ge showing energy, ℓ -transfer, spectroscopic factor, and sample spectrum for states populated in the (p,d) reaction.

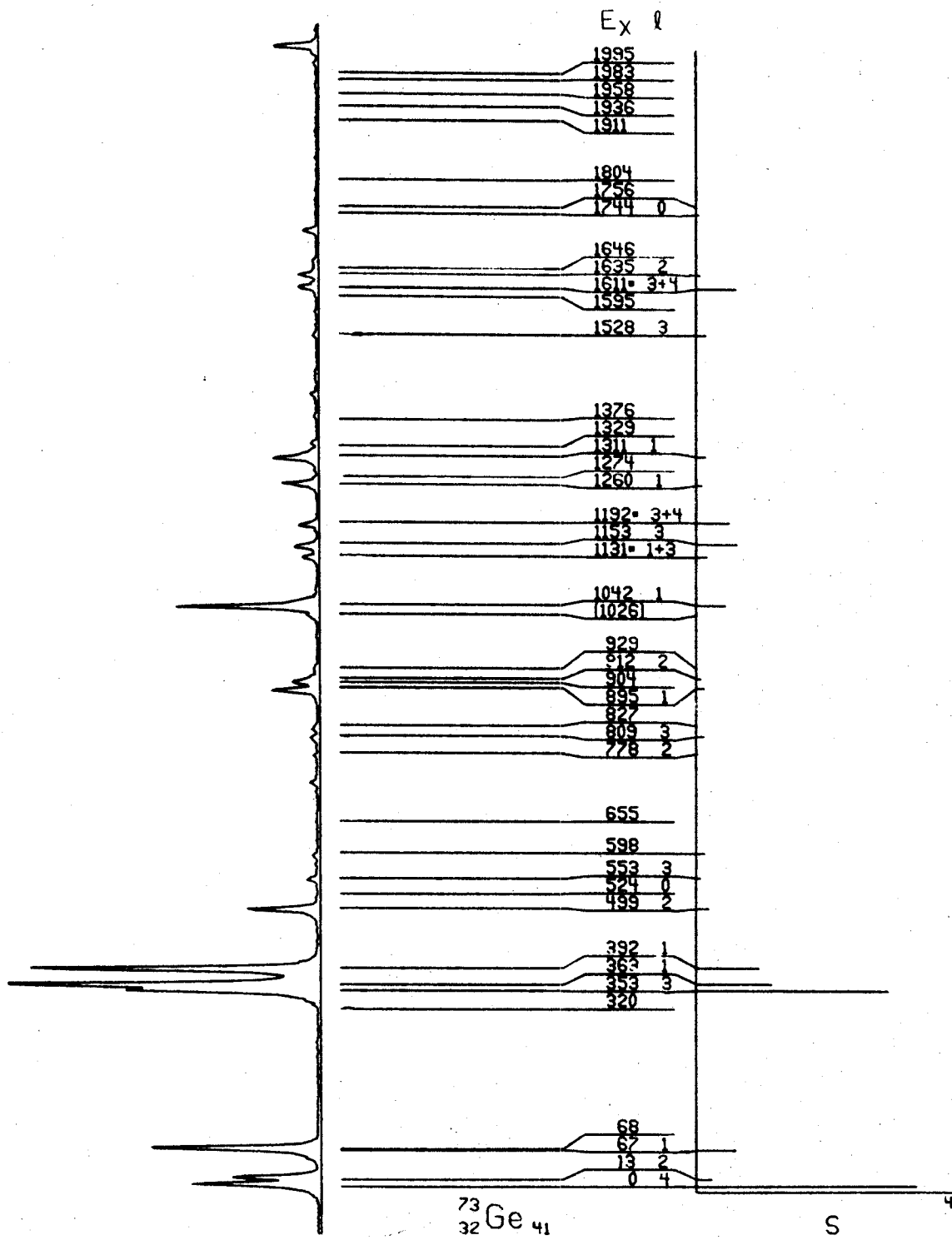


Figure 20

Figure 21. Energy level diagram for states below 2 MeV in ^{75}Ge showing energy, ℓ -transfer, spectroscopic factor, and sample spectrum for states populated in the (p,d) reaction.

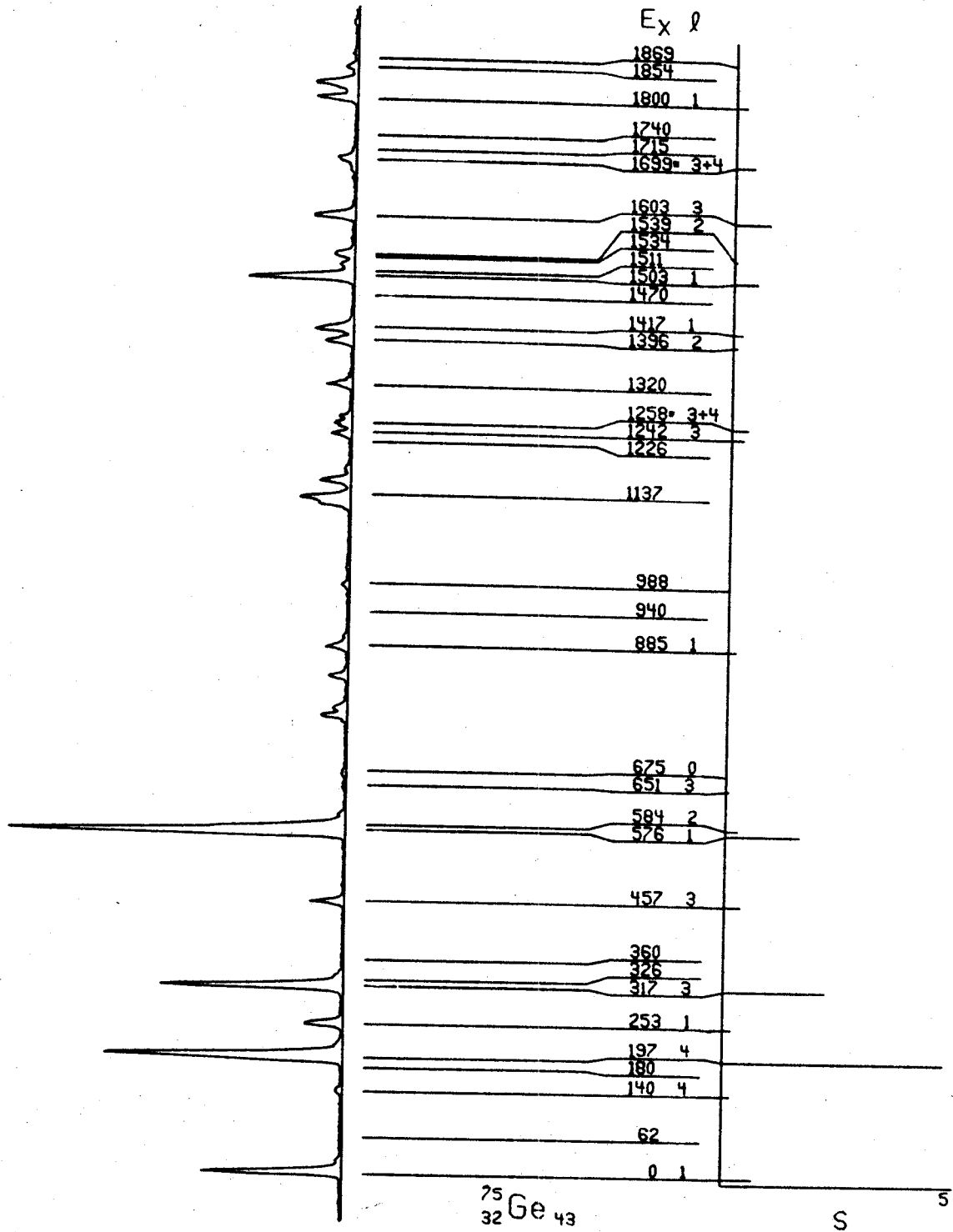


Figure 21

nuclei $T_z = (n-z)/2$, and usually $T = T_z$ for the states of low excitation energy. Thus, ^{69}Ge has $T_z = 5/2$, while the ground state of ^{70}Ge has $T_z = 3$, etc. The above relation for T_z holds for individual protons and neutrons also, so that for protons $T_z = -1/2$ and for neutrons $T_z = 1/2$.

Consider ^{70}Ge which has 4 active protons and 10 active neutrons and see what happens to T for proton and neutron pickup. For proton pickup we have an initial isospin $T^i = 3$ and $T_z^i = 3$ coupled to a proton isospin $T^P = 1/2$ and $T_z^P = -1/2$ to give a final isospin T^f and T_z^f .

The following relations must hold:

$$T_z^f = T_z^i - T_z^P \quad 1)$$

$$T^f = T^i \pm T^P \quad 2)$$

$$T^f \geq T_z^f \quad 3)$$

Thus, $T_z^f = 7/2$ and $T^f = 7/2$ since $T^f = 5/2$ does not satisfy the last relation above. Now the sum-rule for the pickup of the 4 active protons is

$$C^2(7/2, 7/2) \Sigma S(3-7/2) = 4$$

In this equation $C^2(7/2, 7/2)$ is the Clebsch-Gordon coefficient for $T = 3$, $T_z = 3$ coupled to $T = 1/2$, $T_z = -1/2$ to give $T = 7/2$,

$T_z = 7/2$, and $\Sigma S(3-7/2)$ is the sum of all spectroscopic factors for proton pickup transitions from ^{70}Ge .

Neutron pickup is slightly more complicated. Using Equations 1-3 above we find $T_z^f = 5/2$ and both $T^f = 5/2$ (called $T_<$) and $T^f = 7/2$ (called $T_>$) are allowed. It will be noted that a $T_>$ state will have the same isospin as states populated by proton pickup only with a different z-projection. Indeed there will be pairs of states populated in proton and neutron pickup whose wave functions differ only in T_z . These are said to be analogue states. The sum-rule for neutron pickup has two terms, one for $T_>$ states and one for $T_<$ states. Since we have 10 active neutrons in ^{70}Ge it takes the form:

$$c^2(5/2, 7/2) \Sigma S(3-7/2) + c^2(5/2, 5/2) \Sigma S(3-5/2) = 10.$$

In this equation $\Sigma S(3-7/2)$ is the same as for proton pickup so that it can be calculated from the proton pickup limit equation and used to calculate the limit for $T_<$ states in neutron pickup. This is useful for our analysis since all the $T_>$ states in the germanium nuclei are calculated to be at greater than 9 MeV excitation energy and are therefore unobserved in our experiment. Using this procedure we obtain the limits listed in Table 7. Also listed in Table 7 are the summed spectroscopic factors for each ℓ -transfer in each reaction. For each reaction the total sums are very close to the sum-rule limits.

Table 7. Summed spectroscopic factors.

Reaction	$^{70}\text{Ge}(p,d)$	$^{72}\text{Ge}(p,d)$	$^{73}\text{Ge}(p,d)$	$^{74}\text{Ge}(p,d)$	$^{76}\text{Ge}(p,d)$
l -transfer					
0	.03	.06	.01	.03	.02
1	3.32	3.64	3.69	3.96	3.92
2	.15	.20	.49	.60	.38
3	6.22	5.4	6.37	4.10	4.65
4	1.69	2.06	1.32	4.81	5.66
total	11.50	11.50	11.90	13.55	14.80
limit	9.43	11.56	12.60	13.64	15.69

While the (p,d) reaction summed spectroscopic factors measure the number of particles in a given orbit, the (d,p) reaction summed spectroscopic factors measure the number of holes in (or emptiness of) a given orbit. Therefore, if the emptiness measured by the (d,p) reaction is added to the fullness measured by the (p,d) reaction, the result should be 1. Table 8 presents such a comparison between our data on the even targets and the (d,p) results of Goldman¹⁴⁾ and of Kato.¹⁶⁾ In general, the agreement is quite good and indicates that 75-100% of the allowed strength has been observed. Following are comments on each orbit:

1f_{5/2} orbit: Neither Kato¹⁶⁾ nor Hasselgren³⁾ observed an $\ell=3$ transition in the $^{76}\text{Ge}(d,p)$ reaction. This would indicate that the 1f_{5/2} orbit is full in the ground state of ^{76}Ge . Our results indicate that it is only about 80% full, but it may be that we do not see all the $\ell=3$ strength as we would expect some $\ell=3$ transitions to higher excited states. For ^{70}Ge there is clearly too much strength observed. However, Goldman's data¹⁴⁾ shows only one definite $\ell=3$ transition in the (d,p) reaction and that one was mixed with an $\ell=4$. Due to the poor quality of the (d,p) data there must be a very large uncertainty attached to extracting spectroscopic factors from mixed- ℓ doublets. It, therefore, seems likely that the (p,d) strength is at least approximately correct.

2p_{3/2} and 2p_{1/2} orbits: For these strengths there is the difficulty of making accurate spin assignments which

Table 8. Fractional fullness (from (p,d)) and emptiness (from (d,p)) of orbits.

		$^{70}\text{Ge}^{\text{a}}$	^{72}Ge	^{74}Ge	^{76}Ge
$1f_{5/2}$	(p,d)	.85	.90	.82	.78
	(d,p)	.70	.18	.20	0.0
	sum	1.55	1.08	1.02	.78
$2p_{3/2}$	(p,d)	.50	.69	.81	.73
	(d,p)	.03	.14	.13	.06
	sum	.53	.83	.94	.79
$2p_{1/2}$	(p,d)	.36	.43	.36	.49
	(d,p)	.50	.50	.38	.26
	sum	.86	.93	.74	.75
$1g_{9/2}$	(p,d)	.14	.21	.40	.57
	(d,p)	.70	.51	.43	.32
	sum	.84	.72	.83	.89
$2d_{5/2}$	(p,d)	.02	.03	.09	.06
	(d,p)	.50	.66	.70	.58
	sum	.52	.69	.79	.64
$3s_{1/2}$	(p,d)	.01	.03	.02	.01
	(d,p)	.50	1.06	.93	.89
	sum	.51	1.09	.95	.90

^{a)} (p,d) data has been normalized to sum rule limit.

should be reflected in the summed spectroscopic factors. For example, in $^{70}\text{Ge}(d,p)$ Goldman¹⁴⁾ sees too much $2p_{1/2}$ strength relative to $2p_{3/2}$ strength, but this is due at least partly to incorrect $1/2^-$ spin assignments as discussed previously. It also appears that there should be more $2p_{1/2}$ strength relative $2p_{3/2}$ strength in the $^{74}\text{Ge}(p,d)$ reaction indicating that possibly some spin assignments are wrong in ^{73}Ge . In general it appears that 10-25% of the expected $\ell=1$ strength has not been observed in either the (p,d) or (d,p) reactions.

$1g_{9/2}$ orbit: The missing strength here is probably in the (d,p) reaction, as $\ell=4$ transitions in the (p,d) reaction should populate low-lying states.

Some of the missing strength noted above could be due to normalization problems. The absolute spectroscopic factors are probably only accurate to 15 or 20% and this could account for some of the discrepancies.

IX.3 Wave Functions

We will now consider what the data tells us about the wave functions of these nuclei. Based on the simplest shell model picture we would expect to see the $1f_{5/2}$ and $2p_{3/2}$ orbits filled for the ground states of all the target nuclei. ^{72}Ge would also have the $2p_{1/2}$ orbit filled and for the higher A targets the $1g_{9/2}$ orbit would begin to fill up to 4 particles for ^{76}Ge . However, this picture does not take into account

the binding energy that comes in when two nucleons in the same orbit pair their spins to produce a net sum of zero angular momentum. This pairing energy can change the order of filling in the following way. If, for example, the pairing energy of two nucleons in the $1g_{9/2}$ orbit is greater than twice the difference in energy between the $1g_{9/2}$ and $2p_{1/2}$ orbit, two nucleons will populate the $1g_{9/2}$ orbit rather than the $2p_{1/2}$ orbit. Also, the simple model is based primarily on a calculation of the order of the orbits and since these orbits are very close to each other their order may be different in some nuclei.

The spectroscopic factors give us a measure of the actual population of the different orbits and a better idea of what the wave functions look like. The wave function will actually be a linear combination of all the possible arrangements of the active particles in the active space. In general, our data give us no information about the proton structure. However, the fact that we see most of the previously observed states for these nuclei indicates that to a good approximation all the protons can be considered part of the core. The data also indicates that for these nuclei we can consider all the neutron orbits up through the $1f_{7/2}$ orbit as filled and constituting the remainder of the core nucleons. This leaves ten active neutrons in ^{70}Ge . The active space includes the $1f_{5/2}$, $2p_{3/2}$, $2p_{1/2}$, $1g_{9/2}$, $2d_{5/2}$, and $3s_{1/2}$ orbits. The summed strengths measured for these orbits

place restrictions on their populations. In particular, the small $2d_{5/2}$ and $3s_{1/2}$ strengths indicate that these orbits are only weakly populated and perhaps, to a good approximation, terms containing them could be ignored. The fact that they are populated at all indicates that in these nuclei they must be much closer in energy to the $1g_{9/2}$ orbit than predicted by the simple shell model calculation. On the other hand, the $1f_{5/2}$ orbit is mostly full. Thus, in considering terms for the wave function, we could ignore those with a small $1f_{5/2}$ population. If we made the above approximations, and assumed that the $1f_{5/2}$ orbit always contains at least four particles, we could write down the wave function for ^{70}Ge as follows:

$$\begin{aligned}
 ^{70}\text{Ge} = & c_1(1f_{5/2})^6(2p_{3/2})^4 + c_2(1f_{5/2})^6(2p_{3/2})^2(2p_{1/2})^2 \\
 & + c_3(1f_{5/2})^6(2p_{3/2})^2(1g_{9/2})^2 + c_4(1f_{5/2})^6(2p_{1/2})^2(1g_{9/2})^2 \\
 & + c_5(1f_{5/2})^6(1g_{9/2})^4 + c_5(1f_{5/2})^4(2p_{3/2})^4(2p_{1/2})^2 \\
 & + c_7(1f_{5/2})^4(2p_{3/2})^4(1g_{9/2})^2 \\
 & + c_8(1f_{5/2})^4(2p_{3/2})^2(2p_{1/2})^2(1g_{9/2})^2 \\
 & + c_9(1f_{5/2})^4(2p_{3/2})^2(1g_{9/2})^4 \\
 & + c_{10}(1f_{5/2})^4(2p_{1/2})^2(1g_{9/2})^4 \\
 & + c_{11}(1f_{5/2})^4(1g_{9/2})^6.
 \end{aligned}$$

The summed spectroscopic factors place restrictions on the coefficients, but we do not have enough information to

determine them uniquely. For example, since the summed $2p_{1/2}$ strength is .72 we can write down the following restriction:

$$.72 = 2C_2^2 + 2C_4^2 + 2C_6^2 + 2C_8^2 + 2C_{10}^2.$$

Similar relations could be written down for the summed strength for each orbit. This would give us four equations with eleven unknowns. We can say that terms involving $(lg_{9/2})^6$ and $(lg_{9/2})^4$ must have small coefficients since the summed strength for the $lg_{9/2}$ orbit is only about 1.4. Similar wave functions could be written down for each of the target nuclei but in order to completely determine the coefficients one must use the information contained in the excitation energies of the excited states. This requires a complete shell model calculation.

For the excited states in the odd nuclei we only have information about their wave function relative to the target wave function. In each odd nucleus there is a low lying state that carries almost all the $\ell=4$ strength for that reaction. This indicates that the wave functions for these $9/2^+$ states are just the same as the target wave function with a $lg_{9/2}$ neutron removed. Similar arguments hold for the strongly populated $5/2^-$, $3/2^-$, and $1/2^-$ states. The other excited states have wave functions which differ more significantly from the target wave function.

Fournier et al.¹⁸⁾ have tried to do a very simple

calculation assuming that only the $2p_{1/2}$ and $1g_{9/2}$ orbits are involved in the active space. Based on the summed spectroscopic factors, this appears to be too much of an over simplification to yield any useful information. While it might be possible to consider the $1f_{5/2}$ orbit as full, it is clear that the $2p_{3/2}$ orbit must be taken as part of the active space.

IX.4 Order of Filling of Orbits

The summed spectroscopic factors also give us some information about the order in which the orbits are filling as we add neutrons in the germanium isotopes. Due to the small population of the $2d_{5/2}$ and the $3s_{1/2}$ orbits we cannot say much about them except that the $2d_{5/2}$ orbit is gaining some population as we go from ^{70}Ge to ^{76}Ge . This leaves the $2p_{3/2}$, $2p_{1/2}$, $1f_{5/2}$, and $1g_{9/2}$ orbits for consideration. For the even isotopes the $1f_{5/2}$ orbit maintains a fairly constant population. The apparent decrease exhibited in the spectroscopic factors is possibly due to unobserved $\ell=3$ transitions to higher excited states. The population of the $\ell=1$ orbits increases slightly with the $2p_{3/2}$ orbit getting most of that increase. The $1g_{9/2}$ orbit is getting most of the overall increase in population which is just what we would expect from the simple shell model picture. The one odd target, ^{73}Ge , shows a deviation from this trend of increasing population of the $1g_{9/2}$ orbit. In this nucleus the $1g_{9/2}$ population is lower than that for ^{72}Ge and the $1f_{5/2}$ population is significantly larger. The apparent decrease in

$1g_{9/2}$ population could be due to $\ell=4$ transitions to highly excited 6^+ and 8^+ states in ^{72}Ge which we do not see, or to some unobserved $\ell=4$ components in states populated by $\ell=2$ transfers.

X. SUGGESTIONS FOR FURTHER STUDY

As has already been mentioned, it would be interesting and helpful to study the J-dependence of the $\ell=1$ transitions with both the (p,d) and (d,p) reactions. In doing this, it would be highly desirable to do the experiment with a counter instead of plates because of the time and effort involved in scanning the plates. Accurate excitation energies are not needed so partial spectra from a small counter would be acceptable. The immediate availability of the data would be very helpful in determining that the experiment is indeed going to be successful before large amounts of time are expended. If the experiments were successful, it would yield accurate spin assignments for more of the states populated by $\ell=1$ transfers and thereby give more information about the wave functions of these nuclei.

The $\ell=3$ J-dependence observed in the nickel region is useful in making spin assignments there, but it cannot be used with confidence in the germanium region since there are no known $7/2^-$ states in these nuclei. A systematic study of the $\ell=3$ angular distributions for the nuclei in the mass region between nickel and germanium might yield more information about the trends in, or existence of, the effect in these nuclei when the $1f_{5/2}$ orbit is more completely filled.

Further spectroscopic information might be gained for the even nuclei by the use of the (p,t) and (p,p') reactions.

Hsu et al.¹⁷⁾ have studied the $^{70}\text{Ge}(p,t)$ reaction but the usefulness of their results was again limited by their energy resolution.

REFERENCES

REFERENCES

1. D. T. Kelly, H. H. Graue, M. W. Greene, and J. F. Sharpey-Schafer, *Bal. Amer. Phys. Soc.* (Jan 1973) 117.
2. A. C. Rester, A. V. Ramayya, J. H. Hamilton, D. Krmpotic, and P. Venugopala Rao, *Nucl. Phys.* A162 (1971) 461.
3. A Hasselgren, *Nucl. Phys.* A198 (1972) 353.
4. Rainer Weishaupt and Dietrich Rabenstein, *Z. Physik* 251 (1972) 105.
5. J. G. Malan, J. W. Tepel, and J. A. M. DeVilliers, *Nucl. Phys.* A143 (1970) 53.
6. J. G. Malan, E. Barnard, J. A. M. DeVilliers, P. van der Merwe, *Nucl. Phys.* A227 (1974) 399.
7. G. C. Salzman, A. Goswami, and D. K. McDaniels, *Nucl. Phys* A192 (1972) 312.
8. K. W. Jones and H. W. Kraner, *Phys. Rev.* C4 (1971) 125.
9. G. Murray, N. E. Sanderson, and J. C. Willmott, *Nucl. Phys* A171 (1971) 435.
10. James R. Van Hise and Albert E. Rainis, *Phys. Rev.* C6 (1972) 6.
11. S. Muszynski, S. K. Mark, *Nucl. Phys.* A142 (1970) 459.
12. Hsuan Chen, P. L. Gardulski, and M. L. Wiedenbeck, *Nucl. Phys.* A219 (1974) 365.
13. David C. Camp. Bruce P. Foster, *Nucl. Phys.* A177 (1971) 401.
14. L. H. Goldman, *Phys. Rev.* 165 (1968) 1203.
15. C. Heyman, P. van der Merwe, I. J. van Heerden, and I. C. Dormehl, *Z. Phys.* 218 (1969) 137.
16. Norihisa Kato, *Nucl. Phys.* A203 (1973) 97.
17. T. H. Hsu, R. Fournier, B. Hird, J. Kroon, G. C. Ball, and F. Ingebretsen, *Nucl. Phys.* A179 (1972) 80.
18. R. Fournier, J. Kroon, T. H. Hsu, B. Hird, G. C. Ball, *Nucl. Phys.* A202 (1973).

19. Computer code written by J. T. Routti, Berkley Radiation Laboratory and adapted for present use by C. B. Morgan, MSU Cyclotron Laboratory.
20. Computer code written by J. A. Rice, MSU Cyclotron Laboratory.
21. A. H. Wapstra and N. B. Gove, Nucl. Data Sec. A, 9 (1971); N. B. Gove and A. H. Wapstra, Nucl. Data Sec. A, 11 (1972)
22. F. D. Becchetti, Jr. and G. W. Greenlees, Phys. Rev. 182 (1969) 1190.
23. Computer code written by P. D. Kunz, University of Colorado.
24. R. C. Johnson and P. J. R. Soper, Phys. Rev. C1 (1970) 976.
25. G. R. Satchler, Phys. Rev. C4 (1971) 1485.
26. Nuclear Data Sheets B1 No. 6 (1966) 80.
27. L. L. Lee, Jr. and J. P. Schiffer, Phys. Rev. 136 (1964) B405.
28. R. Sherr, E. Rost, and M. E. Rickey, Phys. Rev. Letters, 12 (1964) 420.
29. J. A. Nolen, R. G. H. Robertson, and S. Ewald, MSU Cyclotron Annual Report (1972) 23 (unpublished).
30. D. H. Kong, private communication (1974).
31. M. Goldhauer and A. W. Sunyar, Phys. Rev. 83 (1951) 906.